15

Synthesis and Properties of Partially Fluorinated Polyimides for Optical Applications

52

TOHRU MATSUURA, SHINJI ANDO,
and SHIGEKUNI SASAKI

15.1. INTRODUCTION

151.1. Conventional Polyimides

Aromatic polyimides have excellent thermal stability in addition to their good electrical properties, light weight, flexibility, and easy processability. The first aromatic polyimide film (KAPTON, produced by DuPont) was commercialized in the 1960s and has been developed for various aerospace applications. The structure of a typical polyimide PMDA/ODA prepared from pyromellitic dianhydride (PMDA) and 4,4′-oxydianiline (ODA), which has the same structure as KAPTON, is shown in (**1**).[1,2] Aromatic polyimides have excellent thermal stability because they consist of aromatic and imide rings.

Since the invention of integrated circuits (ICs), polyimides as heat-resistant organic polymers have been applied to insulation materials in electronics devices such as flexible printed circuit boards (FPCs), interlayer dielectrics, buffer coatings, and tape automated bonding (TAB). A polyimide thin layer is easily

---

TOHRU MATSUURA, SHINJI ANDO, and SHIGEKUNI SASAKI • Science and Core Technology Group, Nippon Telegraph and Telephone Corp., Musashino-shi, Tokyo 180, Japan. Present address of SHINJI ANDO: Department of Polymer Chemistry, Tokyo Institute of Technology, Meguro-ku, Tokyo 152, Japan.

Fluoropolymers 2: Properties, edited by Hougham *et al.* Plenum Press, New York, 1999.

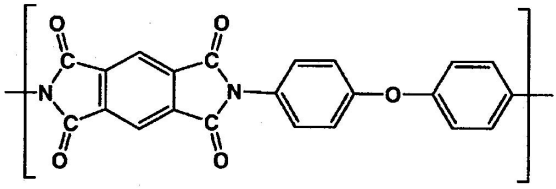

(1)

PMDA/ODA

formed by spin-coating and heat treatment. Flat interlayer surfaces are obtained by solution-coating. This capability is very useful for fabricating multilayer systems, thus enabling high-density integration.[3] Polyimides have been useful materials for insulation and protective layers because of their relatively low fabrication cost and high performance.[4]

However, conventional polyimides such as PMDA/ODA have disadvantages as dielectrics for use in microelectronics, and these polyimides have subsequently been improved by changing their molecular structure. One disadvantage is their high coefficient of thermal expansion (CTE) compared with other materials such as Si and SiO_2. The difference in CTE between polyimides and other materials produces peeling, bending, and cracking in electronic devices. Low-thermal-expansion polyimides can be achieved by a linear polymer backbone and molecular construction with only rigid groups such as phenyl rings and imide rings.[5]

High water absorption is the other problem with insulation materials, because it causes corrosion of metal wiring and instability of electrical properties such as the dielectric constant. Conventional polyimides have relatively high water absorption because of the presence of polar imide rings. However, the water absorption decreases when fluorine is introduced into polyimide molecules because of the former's hydrophobic nature.[6,7]

In addition, miniaturization of electronic devices and components, which achieves high integration and a high signal-propagation speed, is a very important subject in microelectronics. A reduced dielectric constant in insulation materials makes higher integration and a higher signal-propagation speed possible. The high integration also adds to the high signal-propagation speed because of the shorter circuit wiring, but cross-talk occurs as a result of the narrowed wiring gaps. The low dielectric constant of insulation materials also decreases the cross talk. Although conventional polyimides have a relatively low dielectric constant of about 3.5, it can be further decreased by decreasing molecular polarization, and fluorination is one of the best ways to modify polyimides toward this end.[8] A fluorinated polyimide prepared from 2,2-bis(3,4-dicarboxyphenyl)-hexafluoropropane dianhydride (6FDA) and 2,2-bis(4-aminophenyl) hexafluoropropane (4,4′-6F) (**2**) has a low dielectric constant of 2.39 at 10 GHz.[9]

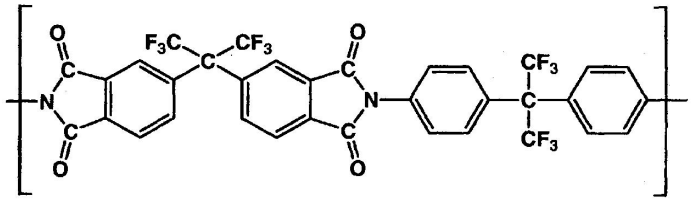

6FDA/4,4'-6F (2)

Several fluorinated polyimides have been synthesized to achieve high-performance materials. Introducing fluorine into polyimides produces a high optical transparency, low refractive index, and solubility, in addition to low dielectrics and low water absorption. 6FDA is the most typical monomer for fluorinated polyimide synthesis.[9–13] Hougham *et al.* have reported the fundamental properties of high-fluorine-content polyimides prepared from 6FDA and various diamines.[8,14,15] Critchley *et al.* have reported polyimides with perfluoroalkylene moieties.[16,17] Many kinds of fluorinated polyimides have been synthesized from pendant-fluorinated diamines,[18,19] 2,2′-bis(trifluoromethyl)-4,4′-diaminobiphenyl (TFDB),[8,14,20–22] perfluoroaromatic diamine,[23] benzotrifluoride-based diamines,[24,25] *o*-substituted diamines,[26] rigid fluorinated dianhydrides,[27-29] 2,2′-bis(fluoroalkoxy)benzidines,[30] and diamines based on trifluoroacetophenone.[31,32]

15.1.2. Optical Applications of Polyimides

A high optical transparency is a basic requirement for optical applications. However, conventional polyimides such as PMDA/ODA have a low optical transparency owing to their dark yellow coloration (they are semitransparent, not opaque). Colorless polyimides have been developed for use in space components, such as solar cells and thermal control systems for the first time.[10]

Light absorption at the visible wavelengths can be explained by electronic charge transfer.[33] Optical transparency increases with decreasing molecular interaction and with shorter intramolecular π-conjugation. St. Clair *et al.* have reported that the fluorinated polyimides with $-C(CF_3)_2-$ and $-SO_2-$ groups have a higher optical transparency compared with nonfluorinated PMDA/ODA.[10] Coloration of polyimides and their electronic charge transfer has been discussed elsewhere.[34]

Recently, optical telecommunications that transmit large amounts of information via light signals have been rapidly replacing conventional electrical telecommunications. Optical polymers, such as poly(methylmethacrylate) (PMMA), polystyrene (PS), and polycarbonate (PC) are used for plastic optical fibers and waveguides. However, these polymers do not have enough thermal

stability for use in optical interconnects. In the near future, optoelectronic integrated circuits and optoelectronic multichip modules will be produced. Materials with high thermal stability will thus become very important in providing compatibility with conventional IC fabrication processes and in ensuring device reliability. Polyimides have excellent thermal stability so they are often used as electronic materials. Furuya *et al.* introduced polyimide as an optical interconnect material for the first time. [35] Reuter *et al.* have applied polyimides to optical interconnects and have evaluated the fluorinated polyimides prepared from 6FDA and three diamines, ODA (**3**), 2,2-bis(3-aminophenyl) hexafluoropropane (3,3′-6F) (**4**), and 4,4′-6F (**2**), as optical waveguide materials.

The polyimides prepared from 6FDA (**2**) and (**4**) have low birefringence. However, their optical loss increases after high-temperature annealing up to 300°C.[36] Furthermore, Sullivan has fabricated high-density optical waveguide components using polyimides to implement optical interconnects.[37] Beuhler and Wargowski have reported that the fluorinated polyimide prepared from 6FDA and 2,2-bis[4-(4-aminophenoxy)phenyl]hexafluoropropane (4-BDAF) (**5**) has low

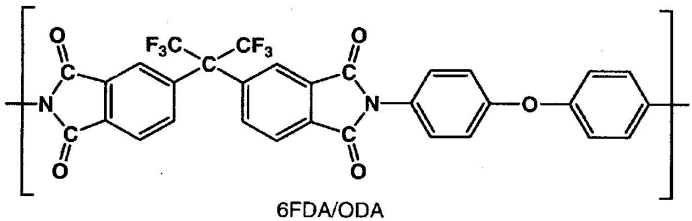

(3)

6FDA/ODA

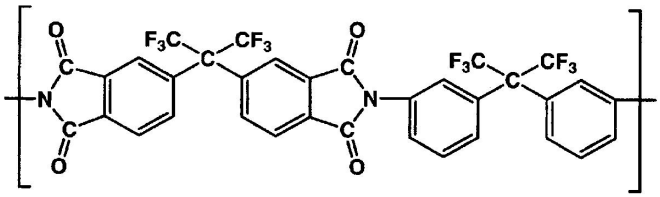

(4)

6FDA/3,3'-6F

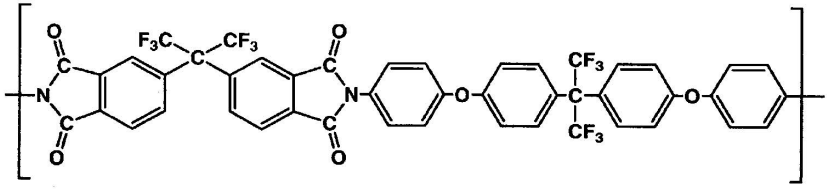

(5)

6FDA/4-BDAF

birefringence ($\Delta n \perp$); however, it is soluble and so cannot be used to fabricate a multilayer structure. They have achieved the fabrication of low-loss buried optical waveguides using 6FDA/4,4′-6F polyimide with a photo-cross-linking group.[38]

15.1.3. Fluorinated Polyimides for Optical Components

With the progress in optical communications, there has been a corresponding demand for the use of polyimides in optical components. Table 15.1 summarizes the primary requirements for optical communication materials and the approach used in this work. Thermal stability above 300°C is required for compatibility with conventional IC fabrication. Polyimides have sufficient thermal stability in addition to easy processability for this use.z

Optical materials are required for high optical transparency at adequate wavelengths for the components. The near-IR wavelengths of 1.3 and 1.5 μm are needed for optical communications (long-distance telecommunication). Most organic polymers, including conventional polyimides, have light absorption based on the vibration of chemical bonds. Indeed, the harmonics of the vibration of carbon–hydrogen (C–H) bonds and oxygen-hydrogen (O–H) bonds are located at the near-IR wavelength. Introducing fluorine instead of hydrogen reduces the light absorption and improves optical transparency in polyimides.[39] On the other hand, the visible wavelengths of 0.63 and 0.85 μm are also needed for local area networks (LANs). Having control of the refractive index and

Table 15.1. Primary Requirements for Optical Components

Requirements for optical process	Requirements for materials	Approach
Compatibility with IC fabrication process	Thermal stability Processability	Selection of polyimide
Low optical loss	High transparency	Introduction of fluorine
Refractive index matching	Precise control of refractive index	Copolymerization
Retardation matching	Control of birefringence	Film elongation
Low stress	Thermal expansion control	Copolymerization
Long-term durability	No Degradation Insensitive to moisture	Introduction of fluorine
Stability against physical impact High-density packaging	Flexibility	Selection of organic polymer
Low-cost fabrication Light weight	Low price Processability	

birefringence is fundamental and important in using optical materials as is optical transparency.

The refractive index must be precisely controlled because it is essential for optical components such as single-mode optical waveguides. This control can be achieved by copolymerization of low- and high-refractive-index polyimides. Birefringence control can be achieved by a film elongation technique using a particular polyimide.

Low stress is important for the optical components, because a high registration rate in device fabrication and good device reliability must be achieved. One cause of stress in device fabrication is the heat cycle of the different materials, which have different CTEs. The stress produced by this difference in CTE causes cracking, peeling, and bending. Furthermore, it also changes the refractive index of materials. Control of thermal expansion is also achieved by copolymerization of low- and high-thermal-expansion polyimides.

Long-term durability is one of the basic specifications for optical components, and polyimides have excellent physical, chemical, and mechanical stability. In practice, optical polymers for applications such as optical waveguides must retain their optical properties and must be reliable in humid environments. Introducing fluorine into polyimides is the most effective way of reducing the water absorption. Organic materials with good flexibility are suitable for stability against physical impact and for high-density packaging. Furthermore, their good processability and low price enable us to make lightweight components at a low fabrication cost.

This chapter describes the synthesis of partially fluorinated polyimides for optical telecommunications applications,[40–42] their optical transparency (optical loss), refractive index, and birefringence properties[43] in addition to their fundamental properties. It also describes their device application as optical interference filters,[44] optical waveplates,[45] and optical waveguides.[46,47]

15.2. SYNTHESIS AND PROPERTIES OF FLUORINATED POLYIMIDES

15.2.1. High-Fluorine-Content Polyimide: 6FDA/TFDB

15.2.1.1. Introducing Fluorine into Polyimides

To achieve a high fluorine content in polyimides, 6FDA and TFDB are selected for polyimide synthesis (Figure 15.1). 6FDA is a typical monomer for fluorine-containing polyimides.[9–13] Polyimides synthesized from 6FDA have a high fluorine content and a flexible structure compared with other conventional polyimides. The other monomer, TFDB,[48,49] is suitable for rigid-rod fluorinated

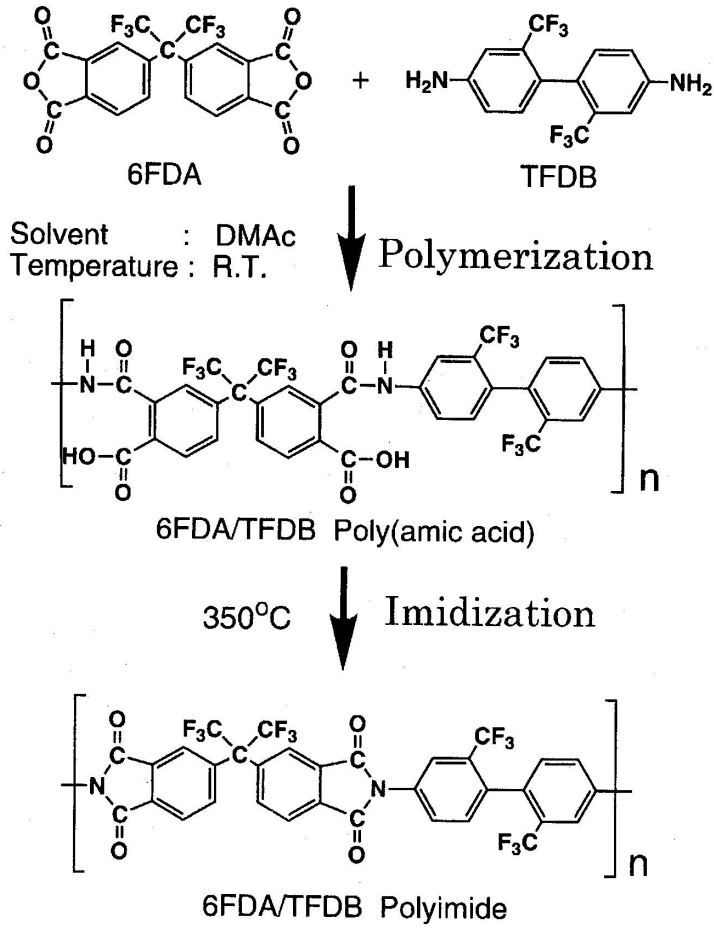

Figure 15.1. Synthesis scheme of high fluorine content polyimide, 6FDA/TFDB.

polyimides. The polyimides prepared from 6FDA have a bent structure, and this causes a slight decrease in the glass transition temperature (T_g). Good thermal stability for high-fluorine-content polyimides is maintained by introducing rigid-rod TFDB units. Harris *et al.* have investigated rigid soluble fluorinated polyimides from TFDB and various tetracarboxylic dianhydrides.[20,22] TFDB also has high polymerization reactivity compared with other fluorinated diamines. Some diamines with fluoro substituents (–F, $–CF_3$, and so on) have low polymerization reactivity, and it is difficult to obtain high-molecular-weight poly(amic acid) using these fluorinated diamines. The strong electron affinity of these fluoro substituents reduces the reactivity of the amino group. However,

TFDB strongly affects the reduction of amino group reactivity by introducing. $-CF_3$ in the meta (*m*-) position. The polymerization reactivity of diamines and tetracarboxylic dianhydrides has been discussed in terms of ^{15}N-, ^{1}H-, ^{13}C-NMR chemical shifts.[5 0]

15.2.1.2. Polymerization and Imidization

The polyimide is synthesized from 6FDA and TFDB by two-step reactions (see Figure 15.1). The first step is polymerization of monomers into poly(amic acid). High-molecular-weight poly(amic acid) is obtained by using equal molar quantities of tetracarboxylic dianhydride (6FDA) and diamine (TFDB). These monomers are dissolved in *N,N*-dimethylacetamide (DMAc) and polymerized into poly(amic acid), also called "polyimide precursor," at room temperature. This poly(amic acid) solution is colorless and of high molecular weight, which gives it a high intrinsic viscosity of more than 1.0 dl/g. The second step is imidization from a poly(amic acid) into a polyimide. The poly(amic acid) solution of DMAc is spin-coated on substrates such as Si and glass, and converted into polyimide film with cyclodehydration and solvent removal by heating to 350°C; 20-μm-thick polyimide films are also colorless in addition to being elastic and flexible.

The imide conversion from poly(amic acid) to polyimide can be observed with NMR spectrometry, as 6FDA/TFDB polyimide demonstrates excellent solubility. Figure 15.2 shows the dependence of imide conversion on curing temperature. The imide conversion is calculated by integrating the intensity ratio

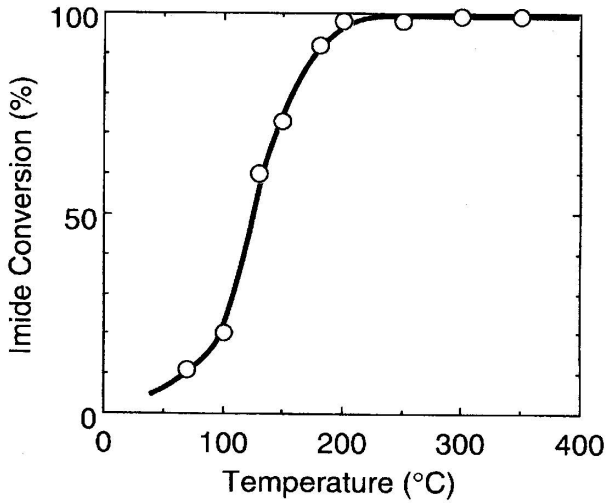

Figure 15.2. Imide conversion from 6FDA/TFDB poly(amic acid) to polyimide by heating.

between the COOH proton peaks at 11 ppm and the aromatic proton peaks from 7.9 to 8.4ppm in high-resolution ^{1}H-NMR spectra imidized at designated temperatures. At 70°C there are the large peaks corresponding to the COOH proton in the poly(amic acid). As the curing temperature rises, the intensity of the COOH proton peaks decreases because the poly(amic acid) converts to the polyimide. When the curing temperature is 180°C the COOH proton peaks almost disappear. This shows that imidization begins at just over 70°C and finishes at about 200°C. At curing temperatures over 200°C, poly(amic acid) is completely converted into polyimide. The imidization process of 6FDA/TFDB poly(amic acid) to polyimide has also been identified by ^{13}C-NMR.[50]

15.2.1.3. Fundamental Properties of High-Fluorine-Content Polyimide

Table 15.2[51] shows the characteristics of the high-fluorine-content 6FDA/TFDB polyimide[40] and KAPTON (nonfluorinated PMDA/ODA type polyimide, DuPont). The T_g of 6FDA/TFDB (335°C) is a little lower than that of PMDA/ODA because of its flexible –C(CF3)2– groups. However, 6FDA/TFDB has a high decomposition temperature of 569°C.

The dielectric constant of dry (0%RH atmosphere) 6FDA/TFDB is as low as 2.8 because of its four trifluoromethyl groups (fluorine content: 31.3%). The low dielectric constant of fluorinated polyimides results from the low electronic polarizability of fluorine-containing groups and the reduced chain–chain electronic interaction.[14,40] An added factor is the additional free volume that can result from fluorine substitution, which can lower the dielectric constant and the refractive index significantly.[15] The dielectric constant of wet (50%RH atmosphere) 6FDA/TFDB, which is 3.0, is a little higher than that of dry 6FDA/TFDB, which is 2.8. It exhibits a slight increase in dielectric constant

Table 15.2. Characteristics of Fluorinated Polyimides

Characteristic	6FDA/TFDB	KAPTON-type H[a] (PMDA/ODA)
Fluorine content (%)	31.3	0
Glass transition temperature (°C)	335	385
Dieletric constant [1 kHz]		
(0% RH)	2.8	3.0
(50% RH)	3.0	3.5
Water absorption (%)	0.2	1.3
Refractive index	1.556	1.78
Coefficient of thermal expansion ($°C^{-1}$)	8.2×10^{-5} (50–300°C)	4.45×10^{-5} (23–400°C)

[a] Source: Toray-DuPont Product Bulletin.[51]

even after being kept in the wet condition. The stability of a dielectric constant is related to water absorption. The water absorption rate of 6FDA/TFDB is very low at 0.2% because of the waterproofing effect of the fluorine atoms, which is lower than that of PMDA/ODA at 1.3%. The stability of the dielectric constant is one of the most important properties for electronic and optical materials.

The CTE of 6FDA/TFDB is a little higher than that of PMDA/ODA. The former has a high CTE because the main chains contain bent hexafluoroisopropylidene units. We discuss the thermal expansion behavior of GFDA/TFDB in the next section, comparing it with the low-thermal-expansion fluorinated polyimide PMDA/TFDB. In addition, the refractive index of GFDA/TFDB, 1.556 at 589.3 nm, is much lower than that of the nonfluorinated PMDA/ODA. This is because of its low electronic polarizability, as well as its low dielectric constant.[15,40]

15.2.2. Rigid-Rod Fluorinated Polyimides: PMDA/TFDB, P2FDA/TFDB, P3FDA/TFDB, and P6FDA/TFDB

15.2.2.1. Molecular Design

Low-thermal-expansion fluorinated polyimides with a rigid-rod molecular structure have been investigated for low stress on substrates such as Si and SiO_2.[41] 6FDA/TFDB has a high fluorine content, but it has a CTE as high as conventional PMDA/ODA. The rigid-rod polyimide main chain was based on the polyimide structure derived from 4,4′-diaminobiphenyl (benzidine) and PMDA. The monomers used in this work are shown in Figure 15.3. In practice, we used the monomer of TFDB as a diamine, which is benzidine with two trifluoromethyl groups. We also used the monomers of 1,4-difluoro-2,3,5,6-benzenetetracarboxylic dianhydride (P2FDA), 1-trifluoromethyl-2,3,5,6-benzenetetracarboxylic dianhydride (P3FDA), and 1,4-bis(trifluoromethyl)-2,3,5,6-benzenetetracarboxylic dianhydride (P6FDA) as tetracarboxylic dianhydrides, which are PMDA with two fluorine and one and two trifluoromethyl groups, respectively.

15.2.2.2. Fundamental Properties

(a) Thermal Expansion Behavior. The CTEs (second run) of the polyimides are shown in Table 15.3. These rigid-rod polyimides exhibit lower CTEs than the fluorinated polyimides already known such as 6FDA/4,4′-6F (CTE = 6.1×10^{-5}°C) prepared from 6FDA and 2,2-bis(4-aminophenyl) hexafluoropropane (4,4′-6F) shown in structure (2), and 6FDA/TFDB. In the polyimides prepared from the same diamines of TFDB or DMDB, the CTE increases as fluorine is introduced and the number of trifluoromethyl side chains in the dianhydride unit increases. In the two polyimides prepared from the same dianhydride of PMDA,

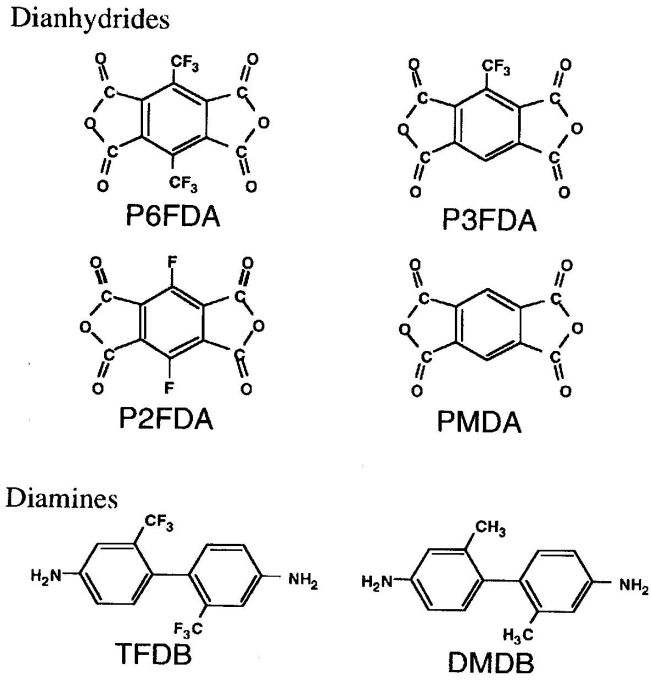

Figure 15.3. Tetracarboxylic dianhydrides and diamines for rigid-rod polyimides.

P3FDA, or P6FDA, the polyimide from DMDB with -CH_3 groups in the diamine unit shows a lower CTE than the polyimides from TFDB with –CF_3 groups. These results suggest that –CF_3 side chains loosen the molecular packing more than the –CH_3 side chain. We have recently reported that the intermolecular packing coefficients of polyimides are considerably decreased by introducing –CF_3 groups from the comparison of the observed calculated refractive indexes.[15,52]

The PMDA/TFDB has a rather low fluorine content of 23.0%; however, its CTE is extremely low at $-5 \times 10^{-6}\ ^{\circ}C^{-1}$. This low-expansion fluorinated polyimide is unique and very useful as a low-thermal-expansion component in optical and electronic materials.

(b) Thermal Stability. Table 15.3 also shows the polymer decomposition temperatures of the polyimides. In the polyimides prepared from the same diamines of TFDB or DMDB, the decomposition temperature decreases as fluorine is introduced and the number of trifluoromethyl side chains in the dianhydride unit increases. The polyimides with –CF_3 groups in the diamine

Table 15.3. Characteristics of Rigid-Rod Fluorinated Polyimides

Polyimide	Fluorine content (%)	CTE [a] ($\times 10^{-5}$ °C^{-1})	Decomposition temperature [b] (°C)	T_g [c] (°C)	Dielectric constant [d] (dry/50%RH)
PMDA/TFDB	23.0	−0.5	613	None detected	3.2/3.6
P2FDA/TFDB	28.2	1.1	540	None detected	
P3FDA/TFDB	30.0	2.8	584	373	2.8/2.9
PGFDA/TFDB	35.7	5.5	496	304	2.6/3.0
PMDA/DMDB	0	−0.1	569	374	
P3FDA/DMDB	12.3	0.5	524	373	
P6FDA/DMDB	21.3	2.2	469	385	
GFDA/TFDB	31.3	8.2	569	335	2.8/3.0

[a] Temperature range, 50–300°C.
[b] 10% weight loss.
[c] Measured by TMA.
[d] Frequency, 1 MHz.

unit have a higher decomposition temperature than those with $-CH_3$ groups. PMDA/TFDB with $-CF_3$ groups in the only diamine unit has produced the highest polymer decomposition temperature in polyimides shown in Table 15.3. The T_gs of all polyimides are higher than 300°C. In particular, T_g s below 400°C are not observed for PMDA/TFDB and P2FDA/TFDB using thermal mechanical analysis (TMA) measurements.

(c) Dielectric Constant and Water Absorption. Figure 15.4 and Table 15.3 show the dielectric constants of the polyimides PMDA/TFDB, P3FDA/TFDB, and P6FDA/TFDB, which have similar molecular structures but different fluorinated substituents. The dielectric constant decreases with increasing fluorine content. The lowest dielectric constant in the dry condition is 2.6 at 1 MHz for P6FDA/TFDB. The low dielectric constants of the fluorinated polyimides result from reduced chain–chain electronic interaction,[8,14] low electronic polarizability of the fluorine, and increased free volume owing to bulky fluorinated groups.[15]

The dielectric constant of polyimide films in the wet condition (50% RH atmosphere) is higher than in the dry condition. This is attributed to water absorption by the polyimides. Figure 15.5 also shows the water absorption of the polyimides, which is due to the presence of imide groups in the polymer [7,53] and decreases with increasing fluorine content because of the hydrophobic effect of fluorine atoms. The water absorption is related to the stability of the dielectric constant. The dielectric constant variability between the dry and wet conditions of highly fluorinated polyimides, P3FDA/TFDB and P6FDA/TFDB, is smaller than

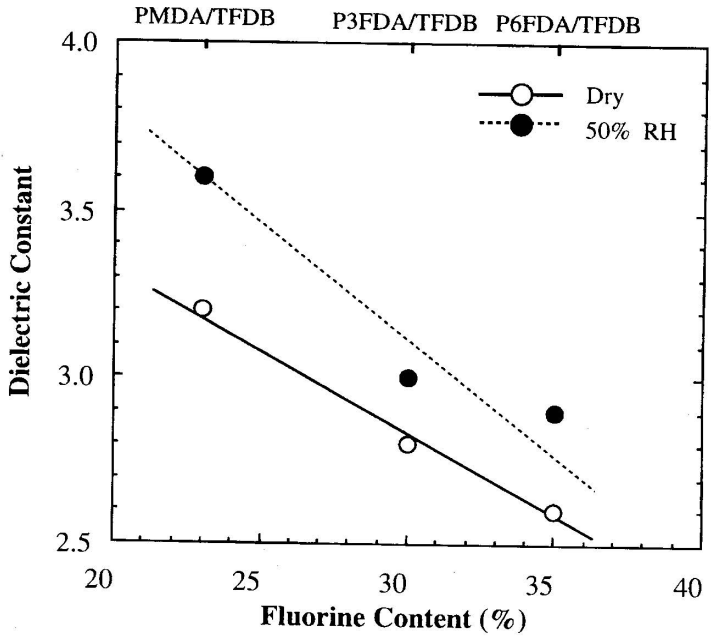

Figure 15.4. Dielectric constant of rigid-rod fluorinated polyimides (frequency —1 MHz).

that of the polyimide with a low fluorine content, PMDA/TFDB. These results indicate that introducing fluorine into the polyimide structure is effective for stabilizing the dielectric constant because of the low water absorption. Stability of the dielectric constant is important for interlayer dielectrics in microelectronic devices.

15.2.3. Fluorinated Copolyimides

15.2.3.1. Property Control for Copolymerization

Controlling the properties of polyimides is very important in applying them to electronic and optical materials, as described in Section 15.1. The difference in CTE between polyimides and other materials causes peeling, bending, and cracking. Furthermore, CTE matching to reduce stress is achieved by precise CTE control. The two different polyimides, GFDA/TFDB with high CTE and PMDA/TFDB with low CTE, are as obtained in previous sections. The CTE of fluorinated polyimides is controlled by copolymerization between high- and low-thermal-expansion polyimides. [42]

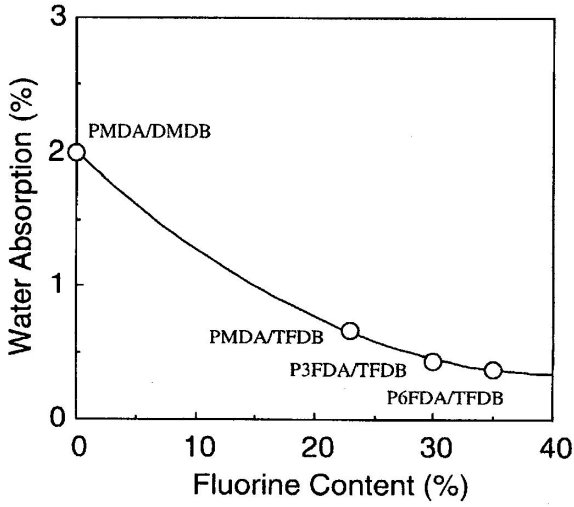

Figure 15.5. Water absorption of rigid-rod fluorinated polyimides,

15.2.3.2. Synthesis of Fluorinated Copolyimides

Figure 15.6 shows the synthesis scheme of fluorinated copolyimides. These copolyimides are synthesized from PMDA, GFDA, and TFDB by two-step reactions. The first step is polymerization of the monomers into copoly(amic acid). High-molecular-weight copoly(amic acid) is obtained by using equal molar quantities of the tetradarboxylic dianhydrides (sum of PMDA and 6FDA) and TFDB. These monomers are dissolved in DMAc and polymerized into poly(amic acid) at room temperature. The second step is imidization from copoly(amic acid) into copolyimide. The copoly(amic acid) solution of DMAc is spin-coated on a substrate and converted into copolyimide film with cyclodehydration and solvent removal by heating to 350°C.

15.2.3.3. Fundamental Properties of Fluorinated Copolyimides

The fluorinated copolyimides (including homopolyimides) are all more transparent than the nonfluorinated PMDA/ODA. The color of 10-μm-thick films changes gradually from bright yellow to colorless as the 6FDA/TFDB content increases. All these copolyimide films are also homogeneous compared with polyimide blends of 6FDA/TFDB and PMDA/TFDB.

The CTE of polyimides decreases with the introduction of a rigid-rod structure into polyimide molecules, and is also controlled by changing the composition of high- and low-thermal-expansion polyimides. Figure 15.7 shows

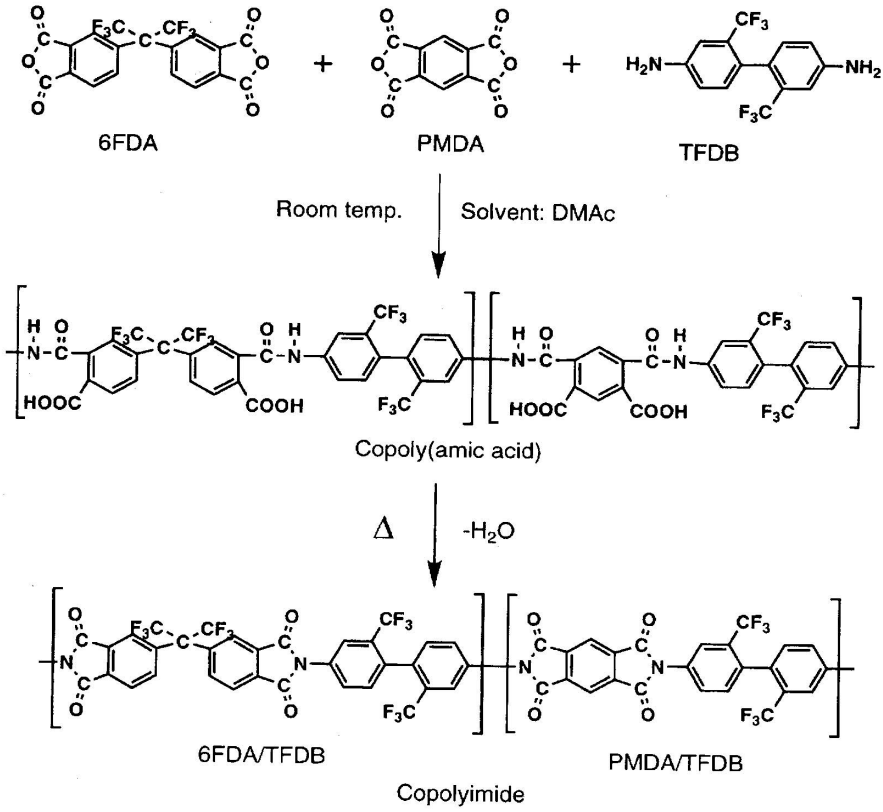

Figure 15.6. Synthesis scheme of fluorinated copolyimides prepared from 6FDA, PMDA, and TFDB.

the CTE of fluorinated copolyimides. PMDA/TFDB polyimide film (6FDA/TFDB content: 0mol%) has a rigid-rod structure and a low CTE of -5×10^{-6} °C^{-1}. On the other hand, 6FDA/TFDB has a much higher CTE of 8.2×10^{-5} °C^{-1}. 6FDA/TFDB is more flexible than PMDA/TFDB, because the bent structure of $-C(CF_3)_2-$—makes the molecular packing in the polyimide film. The CTE values were calculated as the mean between 50 and 300°C. The CTEs of electronic and optoelectronic materials such as SiO_2, Si, Cu, and Al are between those of PMDA/TFDB and GFDA/TFDB. The CTEs of fluorinated copolyimides can be fitted to those of SiO_2, Si, Cu, and Al by changing the 6FDA/TFDB content.

For example, the fluorinated copolyimide with 10 mol% 6FDA/TFDB has almost the same CTE as a Si substrate. Figure 15.8 shows the TMA curves, temperature vs. elongation, of the fluorinated copolyimides with 10 mol%

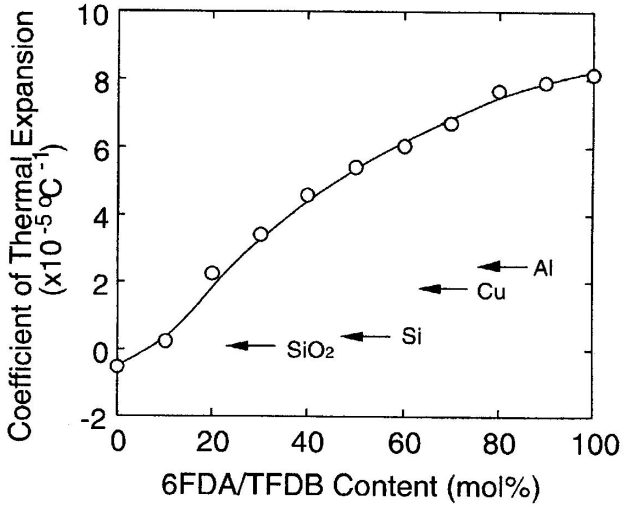

Figure 15.7. Coefficient of thermal expansion of fluorinated copolyimides.

6FDA/TFDB and 100 mol% 6FDA/TFDB. The samples were prepared from poly(amic acid) solutions of DMAc. Each solution was spin-coated on a Si substrate, imidized at 350°C, and peeled from the Si. The TMA curve of the first run is close to that of the second run for the copolyimide with 10mol% 6FDA/TFDB. The copolyimide expands with the Si substrate and has little stress after imidization. On the other hand, the polyimide with 100mol% 6FDA/TFDB has quite different TMA curves for the first and second runs. The elongation of the second run is larger than that of the first run. The stress in 6FDA/TFDB polyimide film is caused by imidization (heating at 350°C), and is released by the TMA measurement of the first run.

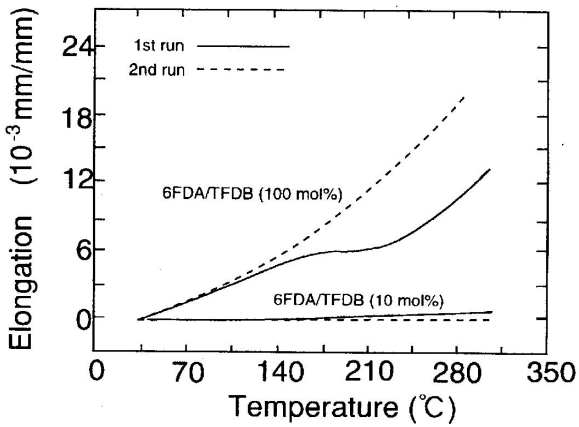

Figure 15.8. TMA curves of copolyimides containing 10 and 100 mol% 6FDA/TFDB.

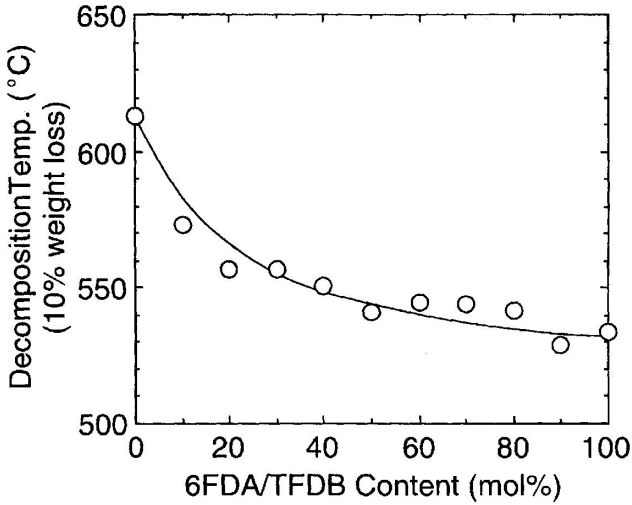

Figure 15.9. Decomposition temperature of fluorinated copolyimides (heating rate—10°C/min).

Figure 15.9 shows the polymer decomposition temperatures of the copolyimides. All have decomposition temperatures defined as 10% weight loss in nitrogen atmosphere, above 500°C. The PMDA/TFDB homopolyimide with 0mol% 6FDA/TFDB content has the highest polymer decomposition temperature at 610°C. The decomposition temperature decreases with increasing 6FDA/TFDB content. Only a small number of 6FDA/TFDB units are required to cause a substantial drop in the decomposition temperature, which is mainly determined by the presence of relatively soft $-C(CF_3)_2-$ groups in the 6FDA/TFDB units.

6FDA/TFDB and PMDA/TFDB homopolyimides have T_gs of 335 and over 400°C (it is not observed below 400°C by differential scanning calorimetry), respectively, and the T_gs of all that have been investigated copolyimides are above 335°C. [37]

It is also possible for these copolyimides to control the refractive index because 6FDA/TFDB and PMDA/TFDB have largely different values. The refractive index and birefringence of the fluorinated copolyimides are described in detail in the next section.

15.3. OPTICAL PROPERTIES OF THE FLUORINATED POLYIMIDES

Three optical properties (optical loss, refractive index, and birefringence) are very important when applying optical polyimides to optical components. These

properties of the fluorinated polyimides and copolyimides are discussed in this section.

15.3.1. Optical Loss

15.3.1.1. Optical Loss in the Visible Region

Introducing fluorine into polyimides is an effective way of improving their optical transparency. The fluorinated polyimides 6FDA/TFDB and PMDA/TFDB and their copolyimides have a high optical transparency at visible wavelengths compared with conventional PMDA/ODA. A 10-μm-thick 6FDA/TFDB polyimide film is colorless after high-temperature heating to 350°C. The transmission UV–visible spectra for several polyimide films are shown in Figure 15.10. 6FDA/DMDB and PMDA/DMDB were synthesized from DMDB, which has a structure containing methyl groups ($-CH_3$) instead of $-CF_3$ in TFDB. The cut-off wavelength (λ_0) of 6FDA/TFDB is lower than that of other polyimides. The degree of optical transparency of the polyimides in the visible region has the following order:

$$\text{6FDA/TFDB} > \text{PMDA/TFDB} = \text{6FDA/DMDB} > \text{PMDA/DMDB}$$

Using the fluorinated monomers 6FDA and TFDB improves optical transparency. 6FDA shows a weaker electron-accepting property than PMDA, and TFDB also shows a weaker electron-donating property. The degree of charge transfer is weakest in 6FDA/TFDB and strongest in PMDA/DMDB. In addition, the –CF3 group reduces intermolecular interaction in polyimides, so 6FDA/TFDB has the highest optical transparency.

The optical losses at a wavelength of 0.63 μm were measured from the scattered light.[54] The experimental setup is illustrated in Figure 15.11. Light from a 0.63-μm helium–neon laser was coupled through a prism into the 10-μm-thick polyimide films on a quartz glass substrate. The light scattered from the film surface was detected by a TV camera. The optical loss was calculated from the plot of the scattered light intensity against the propagation length. The attenuation of scattered light is directly proportional to the optical loss in the polyimide film.

The optical losses of several polyimides are shown in Figure 15.12. 6FDA/TFDB has the lowest optical loss of 0.7 dB/cm of all the polyimides. Both PMDA/TFDB (prepared with PMDA instead of 6FDA) and 6FDA/DMDB (prepared with DMDB instead of TFDB) have a higher optical loss of about 5 dB/cm, and PMDA/DMDB prepared with nonfluorinated PMDA and DMDB has the highest optical loss of 36 dB/cm. The optical loss of polyimide decreases when $-C(CF_3)_2-$ groups are introduced into the polyimide main chain, or when $-CF_3$ groups are introduced into the biphenyl group as the side chain. The relative

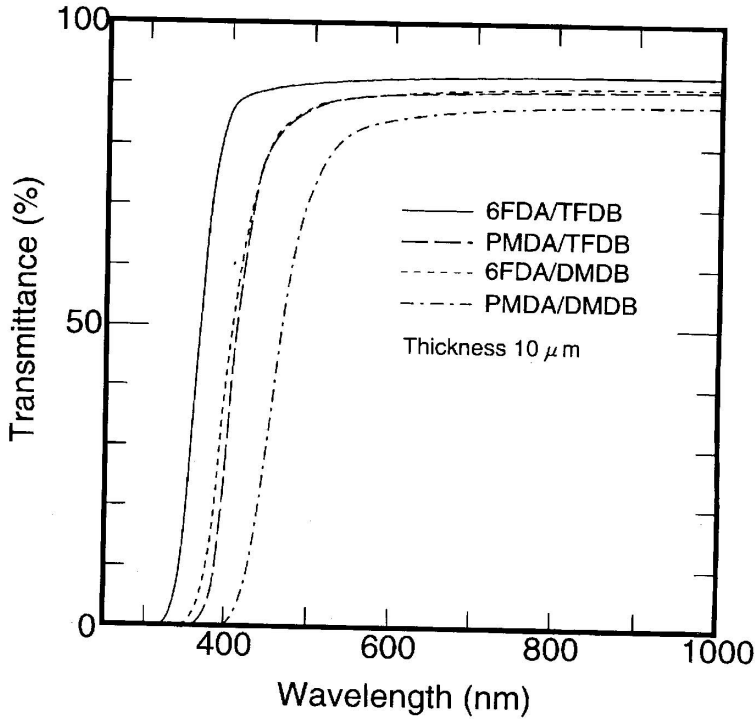

Figure 15.10. UV–visible spectra of various polyimides (film thickness —20 μm).

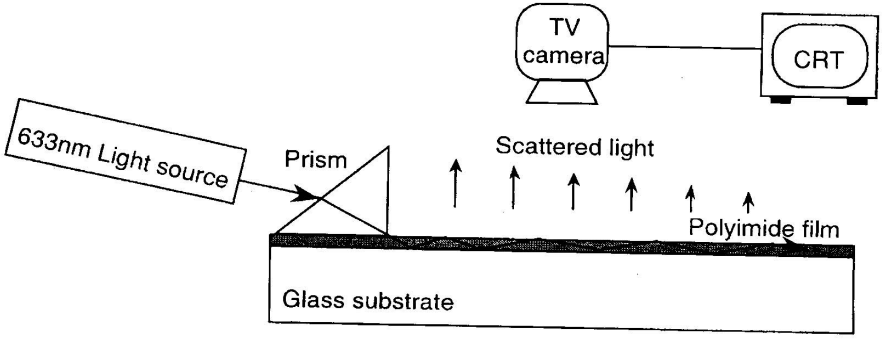

Figure 15.11. Experimental setup for measuring optical loss at 0.63 μm.

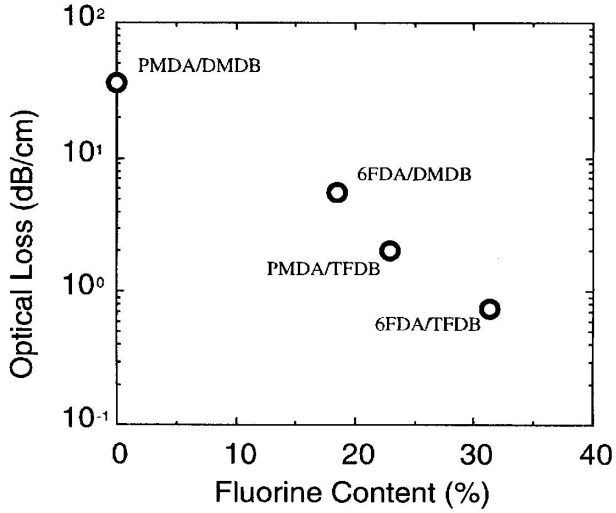

Figure 15.12. Optical loss of various polyimides at 0.63 μm

optical loss of these polyimides agrees well with the coloration and light absorption in the previous section.

The optical loss at the wavelength of 0.63 μm of the copolyimides prepared from PMDA, 6FDA, and TFDB cured at 350°C, shown in Figure 15.13, falls between those of the PMDA/TFDB (4.3 dB/cm) and 6FDA/TFDB (0.7 dB/cm) homopolyimides. The high optical loss with large PMDA/TFDB content results from electronic transition absorption. It decreases monotonically with increasing 6FDA/TFDB content and is not increased by copolymerization. This result indicates that these copolyimides are optically homogeneous and copolymerization of PMDA/TFDB and 6FDA/TFDB does not increase the amount of light scattered at 0.63 μm. On the other hand, the polyimide-blend film prepared from the mixture of 50 wt% 6FDA/TFDB and 50 wt% PMDA/TFDB poly(amic acid) solution could not be measured owing to the large amount of scattered light caused by the inhomogeneity of the polyimide blend.

15.3.1.2. Relation between Optical Loss and Preparation Conditions

The optical loss of polyimides depends on their preparation conditions. Reuter *et al.*[36] have reported the optical loss of commercial fluorinated polyimides in waveguide materials containing two $-C(CF_3)_2-$ groups, 6FDA/3,3′-6F or 6FDA/4,4′-6F, and estimated the optical loss to be below 0.1 dB/cm at 0.63 μm using optimized conditions. However, the loss increases to around 3 dB/cm with a

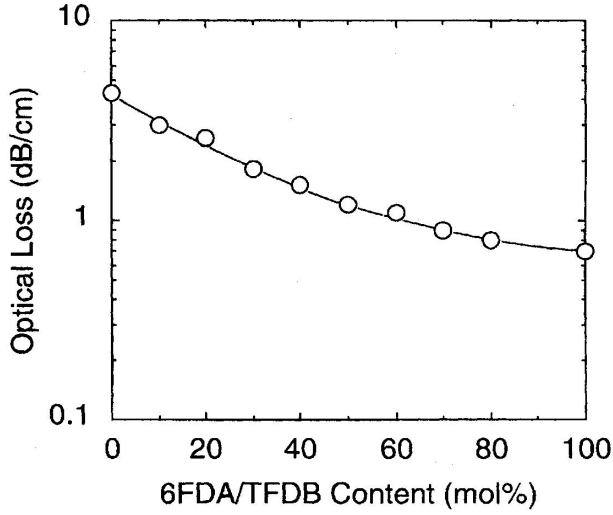

Figure 15.13. Optical loss of fluorinated copolyimides at 0.63 μm.

high curing temperature of 300°C. Optoelectronic applications require polyimides with a low loss and high thermal stability. As described above, the optical loss at 0.63 μm of conventional fluorinated polyimides depends on the curing condition, and increases with increasing curing temperature; however, 6FDA/TFDB has a constant optical loss independent of curing temperature. The optical losses at 0.63 μm of 6FDA/TFDB and PMDA/TFDB for various maximum curing temperatures and in various atmospheres are shown in Figure 15.14. 6FDA/TFDB has a constant optical loss between 250 and 350°C in a nitrogen atmosphere. PMDA/TFDB cured at a low temperature of 250°C has a loss of only 1.3 dB/cm, but it increases with increasing maximum curing temperatures.

The UV–visible spectra of polyimides with different maximum curing temperatures in a nitrogen atmosphere are shown in Figure 15.15. All the 6FDA/TFDB polyimides with different maximum curing temperatures have almost the same absorptions at 0.63 μm. However, for PMDA/TFDB, the absorption at 0.63 μm increases with an increasing maximum curing temperature because the λ_0 is shifted toward longer wavelengths, owing to an increase in molecular packing caused by the high-temperature curing. Compared with PMDA/TFDB, 6FDA/TFDB has less interaction between polyimide molecules owing to the loose packing with the structure containing the $-C(CF_3)_2-$ group after high-temperature curing. These results agree with those for coloration of poly(amic acid) and the polyimide films. In 6FDA/TFDB, the poly(amic acid) films just after solvent removal at 70°C in a vacuum and the polyimide film after

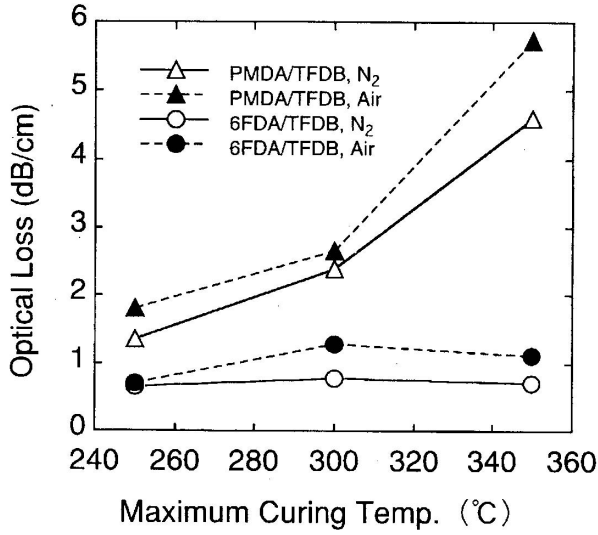

Figure 15.14. Dependence of optical loss at 0.63 μm on the maximum curing temperature.

350°C curing are both colorless. In PMDA/TFDB, however, the poly(amic acid) film before curing is colorless, and the polyimide film after curing is slightly yellow. A similar increase in optical loss at 0.63 μm has also been observed in the fluorinated polyimides 6FDA/3,3′-6F and 6FDA/4,4′-6F. 6FDA/TFDB may have less ordering than 6FDA/3,3′-6F or 6FDA/4,4′-6F polyimides cured at high temperatures above 300°C owing to its higher T_g of 335°C.

For both 6FDA/TFDB and PMDA/TFDB, the optical losses upon curing in a nitrogen atmosphere are lower than those in an air atmosphere. The optical loss increase upon curing in an air atmosphere seems to be caused by a slight oxidative degradation that produces radicals.

15.3.1.3. Optical Loss in the Near-IR Region

The light absorption spectrum measured for the 6FDA/TFDB polyimide film is shown in Figure 15.16. The absorption in the visible region is caused by electronic transition, but the absorption in the near-IR region is mainly caused by the harmonics and their couplings of stretching vibrations of chemical bonds. C–H and O–H bonds strongly affect the absorption in this region. There is an absorption peak that is due to the third harmonic of the stretching vibration of the C–H bond ($3\nu_{CH}^{\phi}$, 1.1 μm), a peak due to the combination of the second harmonic

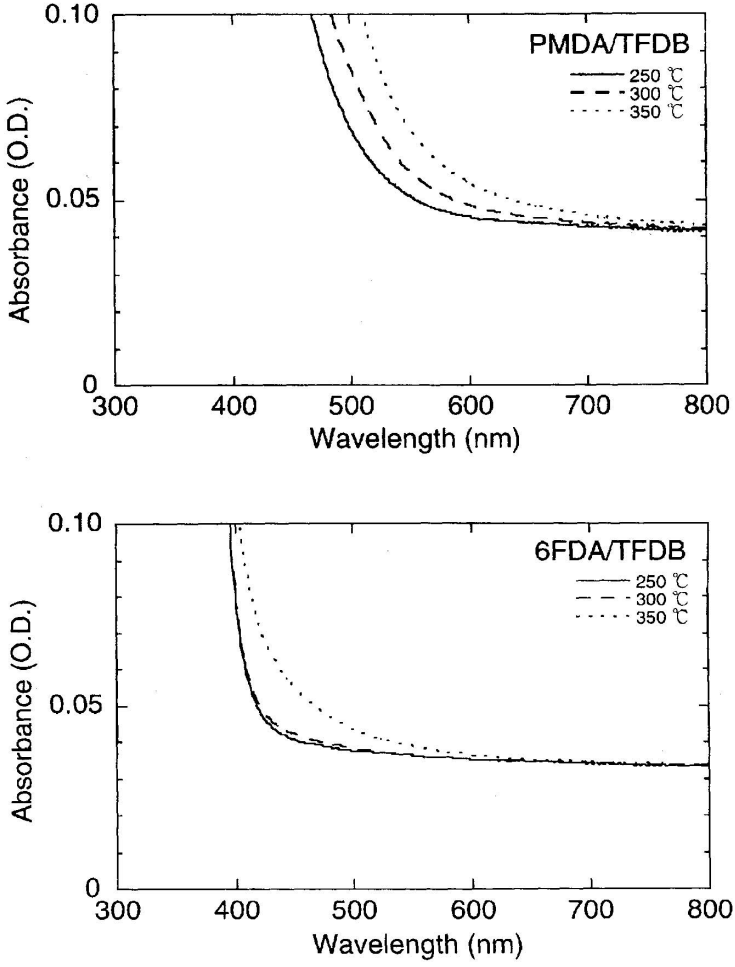

Figure 15.15. UV–visible spectra of polyimides with different cure temperatures

of the stretching vibration and deformation vibration of the C–H bond ($3\nu_{CH}^{\phi} + \delta_{CH}^{\phi}$, 1.4 μm), and a peak due to the second harmonic of the stretching vibration of the C–H bond ($2\nu_{CH}^{\phi}$, 1.65 μm). However, there is little light absorption at the telecommunication wavelengths of 1.3 and 1.55 μm. Furthermore, the number of hydrogen atoms in a unit volume of 6FDA/TFDB is much smaller than for transparent polymers PMMA, PS, and PC, and these hydrogen atoms are only bonded to benzene rings.

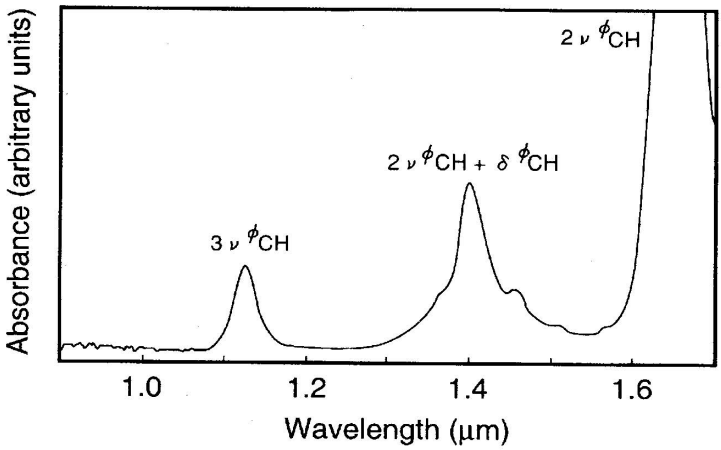

Figure 15.16. Light absorption spectrum of 6FDA/TFDB polyimide film.

The optical loss of a 6FDA/TFDB polyimide block at 1.3 μm was measured directly from the transmission difference between output and input light intensities. The previous optical loss measurement using scattered light could not be done at 1.3 μm because the intensity was very weak. The optical loss without connection loss is 0.3 dB/cm. Apart from the intrinsic material light absorption, there will be an optical loss of 0.3 dB/cm owing to the scattering by voids and fluctuation in the refractive index. The imidization of poly(amic acid) to polyimide with the removal of water may produce voids and refractive index fluctuations, which will degrade transmission.

15.3.2. Refractive Index and Birefringence

15.3.2.1. Refractive Index Control by Copolymerization

The in-plane refractive index (n_{TE}) and out-of-plane refractive index (n_{TM}) at 1.3 μm of 6FDA/TFDB, PMDA/TFDB, and their copolyimides cured at 350°C on a silicon substrate are shown in Figure 15.17 (the refractive index was defined in Section 3.2.3.). The n_{TE} decreases with increasing 6FDA/TFDB content, and can be precisely controlled between 1.523 and 1.614 by changing the 6FDA/TFDB content. In the high-6FDA/TFDB-content region, the slopes of the curves are gentle, and more accurate refractive index control is achieved. The refractive index depends on molecular refraction and molecular volume, and decreases with increasing fluorine content. The n_{TE} decreases with increasing 6FDA/TFDB content, but n_{TM} has a maximum at a 6FDA/TFDB content of

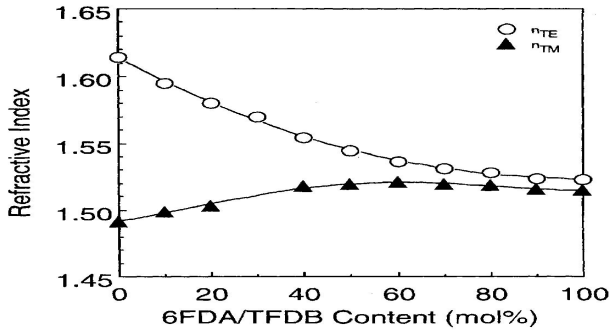

Figure 15.17. Refractive index of fluorinated copolyimides at 1.3 μm.

60mol%. The n_{TM} can also be controlled between 1.514 and 1.521 by changing the 6FDA/TFDB content from 60 to 100 mol%. The n_{TE} is always higher than the n_{TM} for the same 6FDA/TFDB content.

15.3.2.2. Refractive Index Control by Electron Beam Irradiation

The refractive index of fluorinated polyimides increases when they are exposed to electron beam irradiation.[55,56] The degree of refractive index increase can be controlled by adjusting the dose of the electron beam.

Fluorinated polyimide (PMDA/TFDB) and nonfluorinated polyimide (PMDA/DMDB) films prepared on a silicone substrate were introduced into an electron beam lithography system and subsequently exposed for square patterns (4 × 4 mm). The electron beam energy was 25 keV; the beam current was 10 nA, and the beam dose was 300–1500 μC/cm². The 4 × 4 mm square was written by a 0.1-μm-wide electron beam.

Figure 15.18 shows the relationship between the percentage of refractive index increase at the wavelength of 1.3 μm and the electron beam dose for both fluorinated and nonfluorinated polyimides. When the fluorinated polyimide PMDA/TFDB is irradiated the refractive index increased with increasing dose. On the other hand, the refractive index of nonfluorinated polyimide PMDA/DMDB was almost constant when the dose increased. These results show that there is a strong relationship between fluorine content and the increase

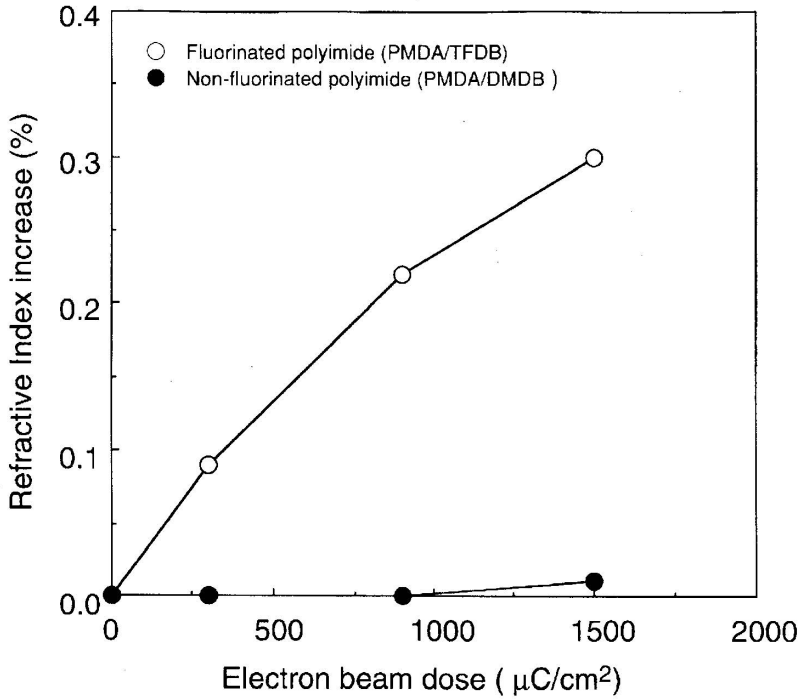

Figure 15.18. Relationship between the percentage of refractive index increase at a wavelength of 1.3 μm and the electron beam dose for both fluorinated and nonfluorinated polyimides.

in refractive index, and the refractive index of fluorinated polyimide can be precisely controlled by changing the electron beam irradiation dose. This increase in refractive index of fluorinated polyimide was due mainly to the elimination of fluorine atoms.

X-ray photoelectron spectroscopy (XPS) was used for surface characterization of both irradiated and nonirradiated fluorinated polyimides. The percentage of fluorine content compared to nonirradiated polyimide decreased 24% for the surface. On the other hand, the other atoms did not change in content after electron beam irradiation. These results show that fluorine atoms were eliminated from fluorinated polyimide by electron beam irradiation.

Figure 15.19 shows the relationship between the percentage of height decrease (Δ) calculated from surface profile measurements and the electron beam dose for both fluorinated and nonfluorinated polyimides. The surface profile between the irradiated and nonirradiated areas was measured. The film shrinks because of electron beam irradiation, and the maximum shrinkage (Δd) reaches up to 0.4% at the film surface.

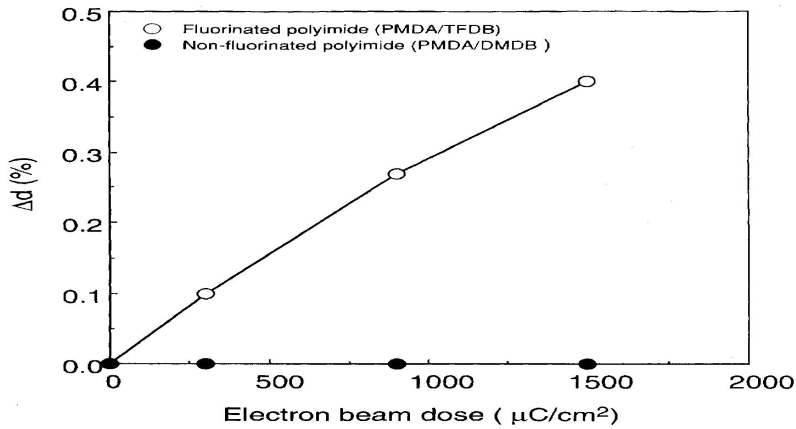

Figure 15.19. Relationship between the percentage of height decrease (Δ) and the electron beam dose for both fluorinated and nonfluorinated polyimides.

The increase in refractive index of fluorinated polyimide is thought to be the result of two main factors: an increase in polarizability because of the elimination of fluorine atoms and an increase in the number of molecules per unit volume because of volume shrinkage.

We attempted to use this increase in refractive index in fabricating polyimide optical waveguides. The fabrication of a fluorinated polyimide waveguide by the direct electron beam writing method is described in Section 4.3.2. We also investigated the changes in the refractive index of fluorinated polyimide films by synchrotron radiation.[5 7] The refractive index at a wavelength of 589.6 nm increased by 1.3% and the thickness decreased by 0.69% for fluorinated polyimide film after 30 min of synchrotron irradiation. From the XPS data the synchrotron radiation leads to production of a fluorine-poor surface.

15.3.2.3. Control of In-Plane Birefringence on Fluorinated Polyimides

Calcite and quartz are commonly used for optical polarization components, such as waveplates, polarizers, and beam splitters. Such inorganic crystals have

good thermal and environmental stability and high optical transparency. However, their birefringence cannot be changed and it is difficult to make them into thin plates or small components. Polymeric materials such as polycarbonates and poly(viny1 alcohol) are also known to be birefringent, but they do not have the thermal or environmental stability needed for use in optical circuits and modules. Thus, there is a strong demand for new optical materials that have a greater, controllable birefringence while having good processability, good tractability, and high thermal and environmental stability.

Figure 15.20 shows schematically refractive index ellipsoids of polyimide prepared on isotropic substrates and uniaxially drawn polyimide. The films prepared on an isotropic substrate have no refractive index anisotropy in the film plane ($n_{\mathrm{TE}_1} = n_{\mathrm{TE}_2}$). However, the in-plane refractive index of the films is always larger than the out-of-plane refractive index ($n_{\mathrm{TE}} > n_{\mathrm{TM}}$). In-plane/out-of-plane birefringence $\Delta n_{\perp}$ can be defined as the difference between n_{TE} and n_{TM}. Thus the films have nonzero $\Delta n_{\perp}$'s when they are prepared on an isotropic substrate. On the other hand, drawing and curing of poly(amic acid) film uniaxially can give an oriented polyimide film with refractive index anisotropy in the film plane ($n_{\mathrm{TE}_1} > n_{\mathrm{TE}_2}$). In-plane birefringence $\Delta n_{||}$ is defined as the difference between the larger and the smaller refractive indexes in the film plane ($\Delta n = n_{\mathrm{TE}_1} - n_{\mathrm{TE}_2}$). Therefore the $\Delta n_{||}$ is not zero for the uniaxially drawn films. Retardation is defined as the product of $\Delta n_{||}$ and the thickness d. In the experiments, the retardation was measured directly by the parallel Nicole rotation method at 1.55 μm (the wavelength for long-distance optical communication), and d was measured from the interference fringe observed in the near-IR absorption spectra.

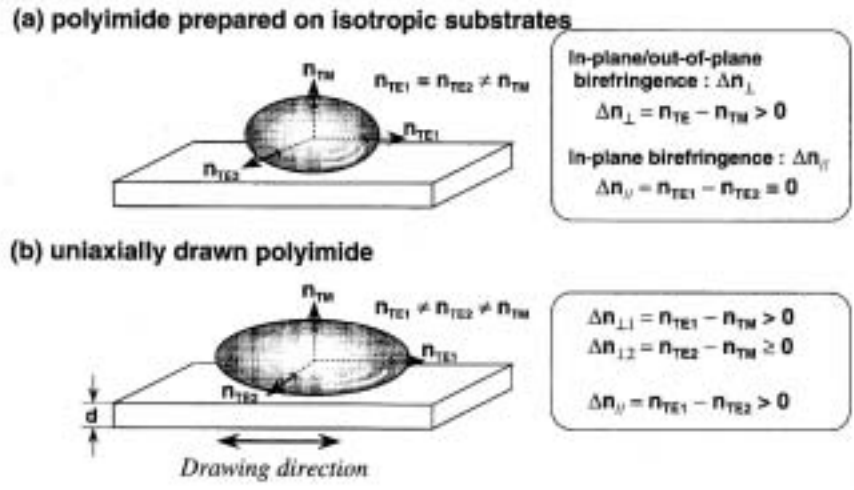

Figure 15.20. Schematic representation of refractive index ellipsoids of: (a) polyimide prepared on isotropic substrates, and (b) uniaxially drawn polyimide.

In order to examine the relationship between molecular structure and in-plane birefringence, six kinds of poly(amic acid) films were prepared. The films were uniaxially drawn during curing with a constant load. Figure 15.21 shows the generated $\Delta n_{||}$ vs. the final curing temperature. The upper three polyimides have rigid PMDA structures, the lower ones have more flexible structures, and the last one is a copolymer of (a) and (e). In general, a rigid-rod structure is accompanied by large polarizability anisotropy along the polymer chain, which causes high in-plane birefringence. The $\Delta n_{||}$ of all the polyimides increases as the final curing temperature is increased, except for 6FDA/TFDB, which shows a very small $\Delta n_{||}$. The polyimides having a PMDA structure show large $\Delta n_{||}$'s. In particular, the rodlike fluorinated polyimide PMDA/TFDB showed the largest $\Delta n_{||}$, which did not saturate even after curing at 460°C. The $\Delta n_{||}$ of this film can be controlled between 0.035 and 0.189 by adjusting the final curing temperature. On the other hand, the flexible polyimides show small $\Delta n_{||}$'s which saturate at lower temperatures.

Thus, PMDA/TFDB was chosen as a novel in-plane birefringent optical material whose birefringence can be precisely controlled. This fluorinated polyimide exhibits low water absorption and a low thermal expansion coefficient.[40] The $\Delta n_{||}$ of this polyimide after curing was linearly proportional to the final curing temperature, heating rate, and load.[58] Figure 15.22 shows the temperature profile and the elongation of the polyimide film. The poly(amic acid) film first begins to shrink at 120°C and then begins to elongate at 180°C. A ^{13}C-NMR examination showed that the imidization reaction became significant at 120°C and was almost complete at 200°C.[50] In-plane birefringence does not occur while the film is shrinking. After imidization is almost complete and the film starts to elongate $\Delta n_{||}$ occurs. As shown in Figure 15.23, $\Delta n_{||}$ shows a linear relationship with the normalized elongation (ΔE) between the most shrunken state at 180°C and the elongated state at the final curing temperature, which coincides with the fact that $\Delta n_{||}$ occurs after the film starts to elongate. These relationships are useful for controlling the $\Delta n_{||}$. Nakagawa reported that uniaxial drawing of UPTON-type poly(amic acid) film can give a highly oriented polyimide film with the largest $\Delta n_{||}$ of 0.18 at 0.633 μm.[58] The maximum $\Delta n_{||}$ of 0.189 at 1.55 μm obtained in this study is considerably larger than this value taking into account the wavelength dispersion of Δn. The estimated $\Delta n_{||}$ of PMDA/TFDB at 0.633 μm is 0.205.[59,60]

15.3.2.4. In-Plane/Out-of-Plane Birefiingence of Polyimides

Aromatic polyimides have many anisotropic imide rings and benzene rings, and they are easy to orient by a film-forming process. Molecular orientation in polyimide films causes in-plane/out-of-plane birefringence ($\Delta n_{\perp}$). Russell et al. have reported the $\Delta n_{\perp}$ of conventional PMDA/ODA.[61] On the other hand, spin-coated polyimide films just after preparation do not cause $\Delta n_{||}$, as noted in the

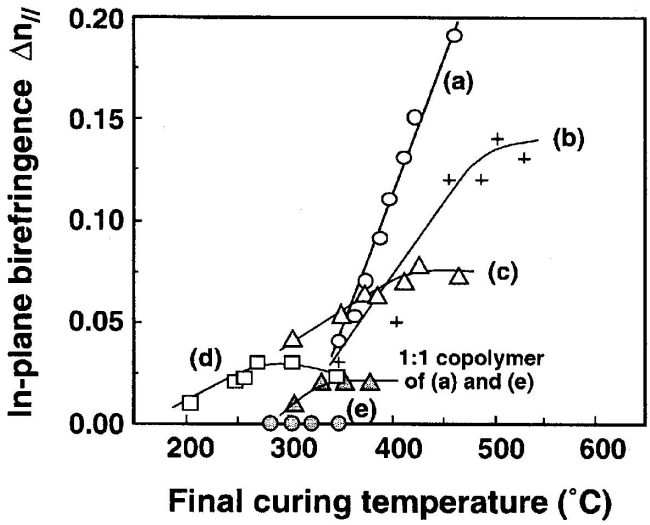

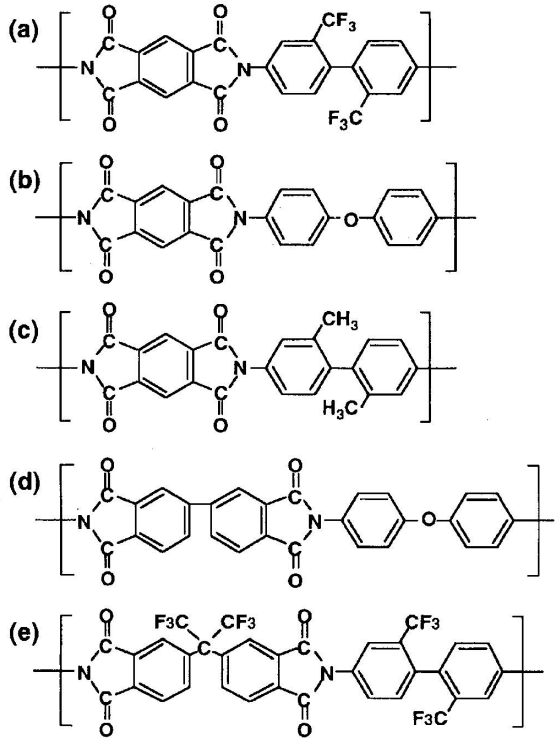

Figure 15.21. Final curing temperature vs. in-plane birefringence of six kinds of polyimides cured under a constant load.

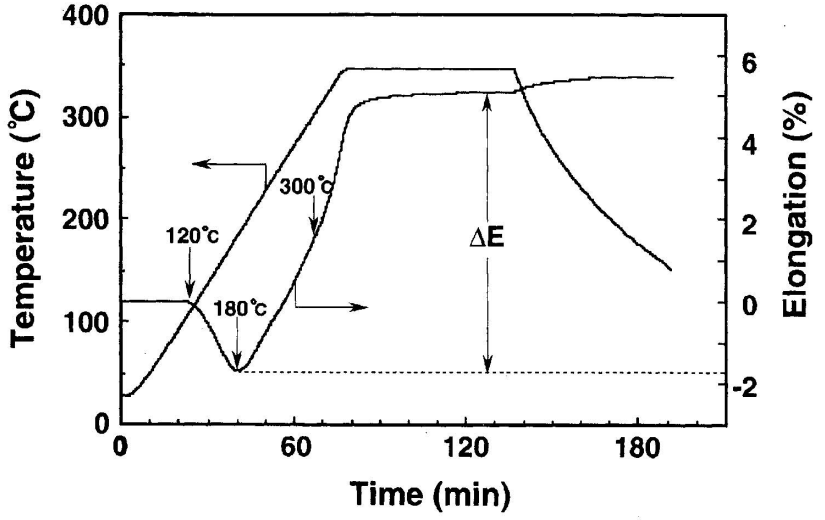

Figure 15.22. Temperature profile and elongation of PMDA/TFDB poly(amic acid) film cured under a constant load.

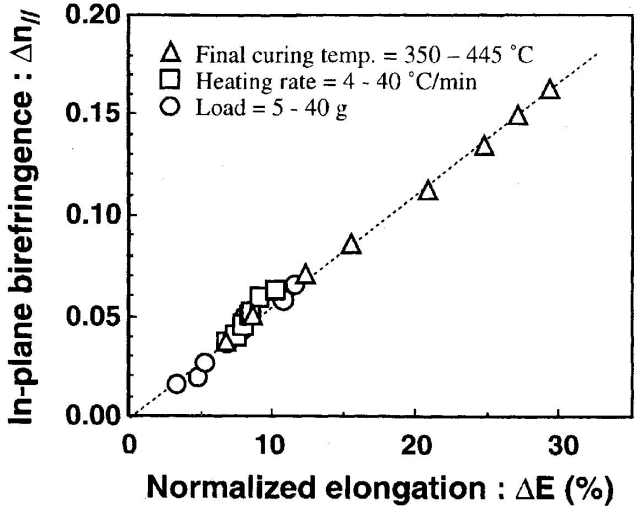

Figure 15.23. Normalized elongation in TMA curves ΔE, vs. in-plane birefringence of polyimide films.

Table 15.4. Birefringence of 6FDA/TFDB Polyimide Film on Si Wafer

Process	Birefringence at 1.3 μm
On Si wafer	0.008
↓	
Removing from Si	0.006
↓	
Annealing at 350°C	0.000

previous section. For polyimide film used as optical material birefringence, like optical transparency and refractive index, is a very important property.

Poly(amic acid) solution is spin-coated on a substrate such as Si, glass, and metals. This coated solution is then converted to polyimide film by heating along with ordering. Furthermore, film stress arises in the final process from high temperature to room temperature with the CTE difference between the polyimide and the substrate, and $\Delta n_{\perp}$ is caused by this orientation and stress.

Table 15.4 shows the $\Delta n_{\perp}$ in each preparation step of annealed 6FDA/TFDB free-standing film. The 6FDA/TFDB polyimide on a Si wafer just after being prepared from the poly(amic acid) solution by heating up to 350°C has a $\Delta n_{\perp}$ of 0.008, which then disappears after removal from the substrate and film-annealing with stress elimination. The birefringence of annealed 6FDA/TFDB film is almost zero.

The $\Delta n_{\perp}$ of fluorinated copolyimides formed on a silicon substrate is shown in the difference between n_{TE} and n_{TM} in Fig. 15.17. The $\Delta n_{\perp}$ decreases with increasing 6FDA/TFDB content. PMDA/TFDB with the largest $\Delta n_{\perp}$ of 0.123 has the linear structure of the phenyl and imide rings in the PMDA unit. They are located in the same plane, and it is easy to align PMDA/TFDB molecules. 6FDA/TFDB, on the other hand, with the smallest $\Delta n_{\perp}$ of 0.008 has the bent structure of two phenyl rings linked by $-C(CF_3)_2-$ groups in the 6FDA unit. The two phenyl rings do not form a coplanar structure. The $\Delta n_{\perp}$ of the copolyimides decreases with increasing 6FDA/TFDB content, and can be controlled between 0.008 and 0.123. There have been some reports on polyimides concerning the relationship between $\Delta n_{\perp}$ and imidization conditions.[58,61]

15.4. OPTICAL APPLICATION OF FLUORINATED POLYIMIDES

15.4.1. Optical Interference Filters on Optical Fluorinated Polyimides

The fluorinated polyimides PMDA/TFDB and 6FDA/TFDB and the copolyimides have the high optical transparency, controllable refractive index,

and controllable birefringence needed for optical materials in addition to a controllable thermal expansion coefficient and thermal stability up to at least 300°C. These fluorinated polyimides are therefore promising materials for optical communication applications.

The fluorinated polyimide has been applied to optical interference filters,[44] and are widely used in optical fiber communication systems. An automatic optical fiber operation support system has been reproduced for optical subscriber lines[62]: It has functions for the remote automatic testing of optical fibers. The filter transmits the communication light (1.3 μm) and blocks the test light (1.55 μm). The test light, which is cut off by the filter in front of the transmission equipment in the user's building, is strongly reflected. Therefore, it is possible to distinguish clearly between line faults and transmission equipment faults by measuring the reflected test light at a telephone office.

The filter is embedded in a slot formed by cutting the optical fiber. The filter must therefore be thin (about 20 μm) to avoid extra loss. A conventional thin filter is made by lapping a thick filter having multilayers of TiO2 and SiO2 on a glass substrate, but this is expensive and difficult to handle. The fluorinated polyimide has a high optical transparency, thermal stability, and tractability to the filter substrate, so it overcomes the problems involved with an optical filter on a glass substrate.

Figure 15.24 shows the fabrication process of the optical filter on a fluorinated polyimide substrate. First, the low-thermal-expansion-coefficient PMDA/TFDB poly(amic acid) solution was spin-coated onto a Si substrate and baked. Then alternate TiO2 and SiO2 layers were formed on the polyimide film by ion-assisted deposition. The multilayered polyimide film was diced and peeled off from the Si substrate. In this way, thin optical filters on a fluorinated polyimide substrate are easily fabricated.

Figure 15.25 shows the transmission spectra of the optical filters on a glass substrate and on a fluorinated polyimide film. The two spectra are very similar, but an optical filter on a fluorinated polyimide is cheaper and easier to handle than one on a glass substrate.

15.4.2. Optical Waveplates

In integrated optics technology, polarization components, such as waveplates, polarizers, and beam splitters, will be reduced in size and incorporated into optical circuits and modules. For example, a small quartz waveplate has been inserted into a silica-based waveguide as a TE/TM mode converter.[5,6] However, one problem with this component is the 5-dB radiation loss resulting from the 92-μm-thick waveplate insertion. Although this considerable loss can be reduced by reducing the waveplate thickness, a calcite half-waveplate, which is about 5 μm thick, is almost impossible to grind and polish because of its fragility.

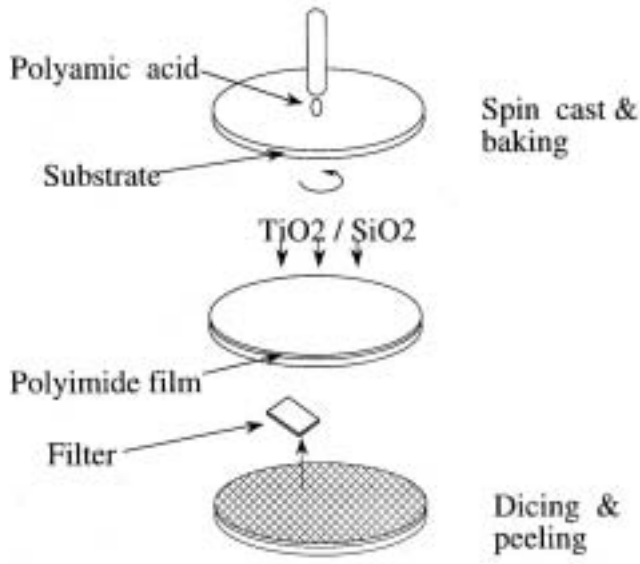

Figure 15.24. Fabrication process of the optical filter on a fluorinated polyimide film.

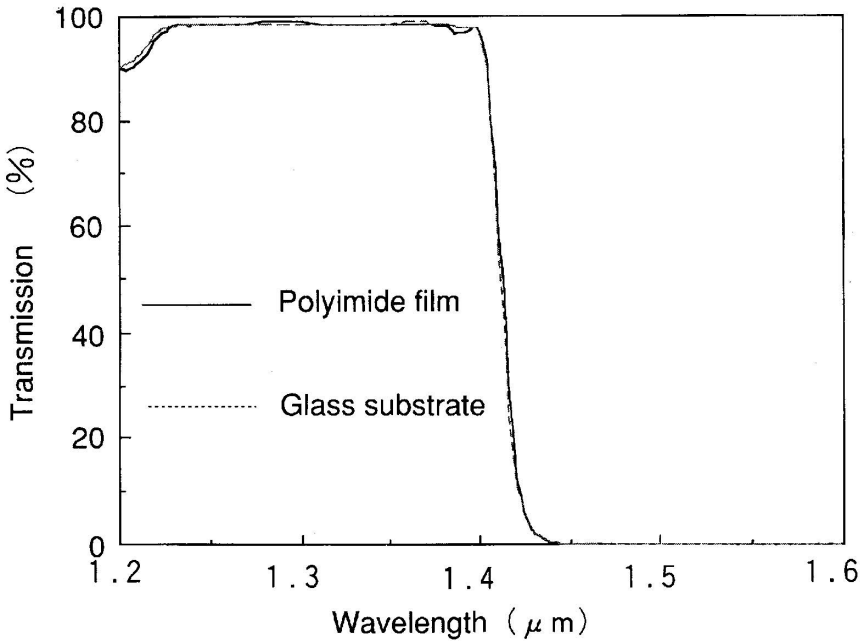

Figure 15.25. Transmission spectra of the optical filters on a fluorinated polyimide film and on a glass substrate.

The function of a half-waveplate is to rotate the polarization direction of optical signals (Figure 15.26). When the optical principal axis is set at 45° to the polarization direction, the polarized light parallel to the substrate (TE polarization) is changed to that perpendicular to the-substrate (TM polarization), and vice versa. Retardation is defined as the product of the in-plane birefiingence $\Delta n_{\|}$ and the thickness, and the retardation of the half-waveplate is set at half the wavelength. In order to reduce the thickness of the half-waveplate, in-plane birefringence should be increased: the birefringence and thickness must be precisely controlled.

In Section 3.2.3. we showed that the rodlike fluorinated polyimide PMDA/TFDB can be used as an in-plane birefringent optical material. The in-plane birefringence of this polyimide can be obtained more easily by curing the poly(amic acid) film with two sides fixed to a metal frame.[59,63] Figure 15.27 shows the tensile stress induced in the film and the retardation measured at 1.55 μm *in situ* during curing. As the temperature increases, polymer chains begin to orient along the fixed direction, generating the in-plane birefringence. This results from shrinkage of the polymer film caused by evaporation of solvent and the imidization reaction. As the TMA curve in Figure 15.22 suggests, the tensile stress was induced only at lower temperatures (45–205°C). However, the retardation increased at the same rate until the final curing temperature, even after the drawing force had disappeared. This indicates that uniaxial tensile stress generates in-plane birefringence at lower temperatures, but the spontaneous orientation of polyimide molecules is the main cause of the birefringence at higher temperatures. This agrees well with the retardation increase that accompanies annealing at temperatures above the final curing temperature of the

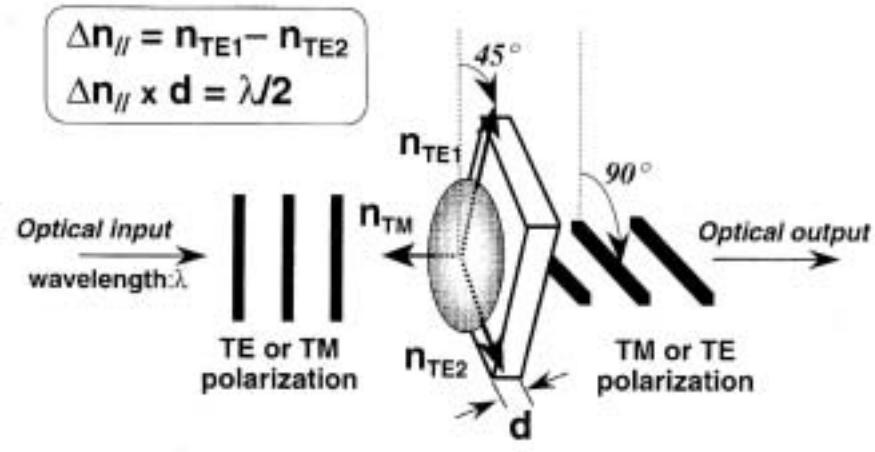

Figure 15.26. Schematic representation of the function of a half-waveplate. It rotates the polarization direction of optical signals by 90°.

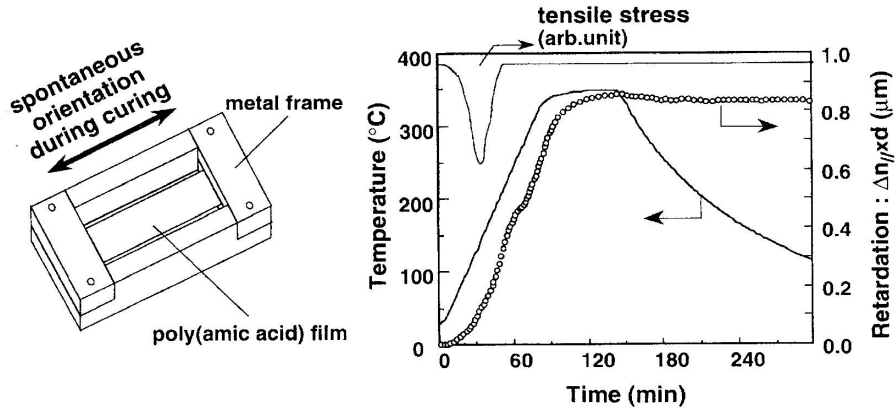

Figure 15.27. Temperature profile, induced tensile stress, and generated retardation of poly(amic acid) film fixed and cured in a metal frame.

polyimide waveplate.[63] The polyimide film elongated about 6% in the fixed direction after the curing at 350°C also suggesting that there is spontaneous orientation.

Since the in-plane birefringence, $\Delta n_{||}$ of polyimides prepared at 350°C is constant (0.053) for thicknesses of 12 to 17 μm, the retardation can be controlled by varying the spinning speed of the poly(amic acid) solutions with an error of less than 1% (Figure 15.28). Thus, a 14.5-μm-thick zeroth-order half-waveplate at 1.55 μm, which is 6.3-fold thinner than a quartz waveplate, was prepared by this method.[64] The retardation of the polyimide waveplate was retained after 1 h of annealing at 350°C, the temperature at which the polyimide is prepared. Figure 15.29 shows the arrayed-waveguide grating multiplexer (AWG) fabricated with silica single-mode buried waveguides. This is one of the wavelength division multiplexers that can be used for lightwave network systems. However, this multiplexer has an undesirable polarization dependence because of waveguide strain birefringence. In order to compensate for this, a polyimide half-waveplate is inserted as a TE/TM mode converter into a groove in the middle of the arrayed waveguides.[64] As a result, the polarization dependence of the AWG multiplexer is completely eliminated. The excess loss caused by the polyimide waveplate was 0.26 dB, which is about 1/20 of that with a quartz half-waveplate.

15.4.3. Optical Waveguides

Low-loss, heat-resistant single-mode optical waveguides were fabricated using the fluorinated copolyimides with a high optical transparency and refractive index controllability. The high thermal stability of these waveguide materials

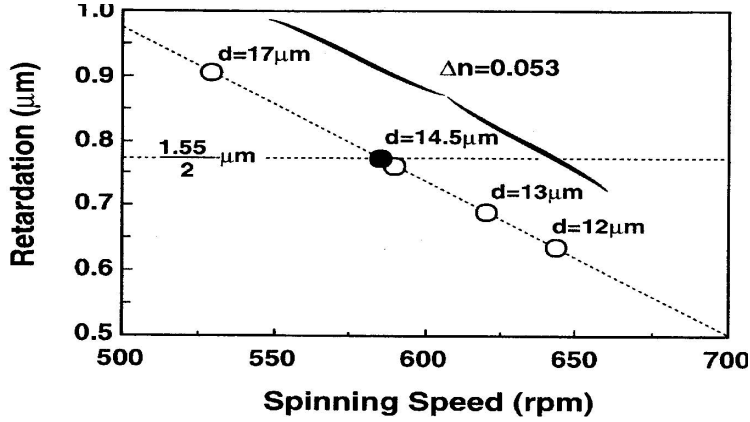

Figure 15.28. Retardation and thickness of polyimides fixed and cured in a metal frame vs. spin-coating speed of poly(amic acid) solution.

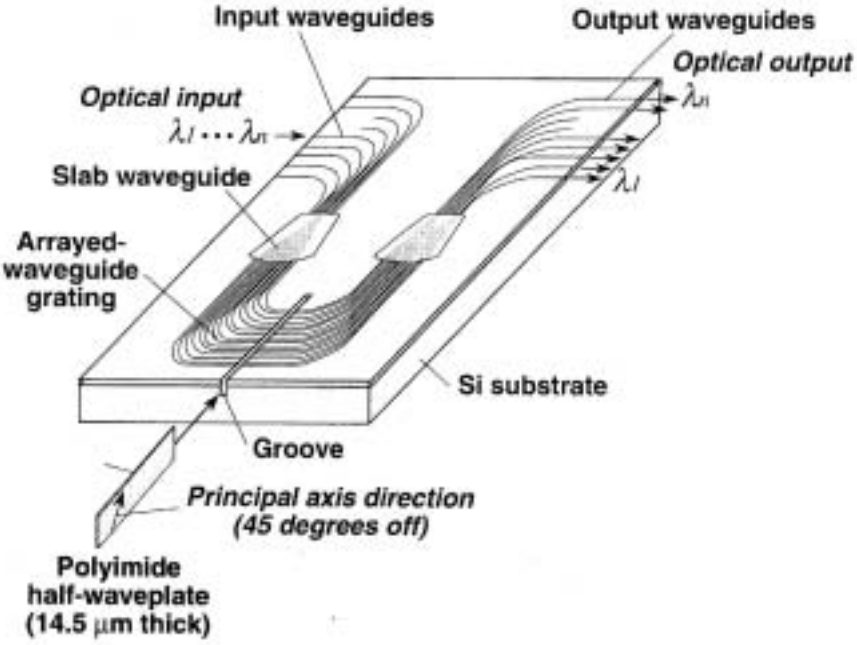

Figure 15.29. Arrayed waveguide grating multiplexer with a thin polyimide half-waveplate.

should allow optoelectronic integrated circuit (OE-IC) fabrication processes and device reliability against heat-cycling.

15.4.3.1. Polyimide Waveguides Using Reactive Ion Etching

(a) Fabrication. Single-mode waveguides were fabricated using polyimides by spin-coating, conventional photolithographic patterning, and reactive ion etching (RIE). [47] Figure 15.30 shows cross-sectional micrographs of the waveguide. The square core (8×8 μm) is completely embedded in the cladding layer. The refractive index difference between the core and cladding is about 0.4%, as measured from the interference micrograph.

Single-mode operation of the waveguides is identified from near-field mode patterns (NFPs). The light intensity of an NFP has a Gaussian distribution with the strongest intensity located at the core center. This waveguide shows single-mode behavior at 1.3 μm.

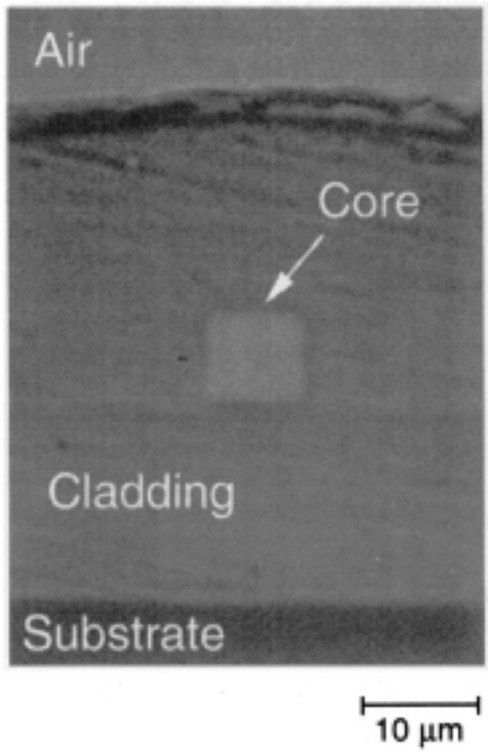

Figure 15.30. Cross-section micrograph of the buried waveguide.

(b) Optical Loss. Figure 15.31 shows the dependence of optical loss (including connection loss for TE polarization) vs. wavelength in the waveguide. This spectrum is mostly similar to those of polyimide materials. The optical loss for light absorption at near-IR wavelengths is mainly due to the harmonics and the couplings of stretching (ν) and deformation (δ) vibrations at chemical bonds such as C–H and O–H bonds. C–H bonds strongly affect the absorption. The wavelengths of 1.3 and 1.55 μm are located in the "windows," and there are no absorption peaks at these wavelengths. This waveguide has a small optical loss of less than 0.3 dB/cm at the telecommunication wavelength of 1.3 μm.[47]

(c) Thermal and Environmental Stability. A film waveguide made from heat-resistant polyimides has high thermal stability. Figure 15.32 shows the optical

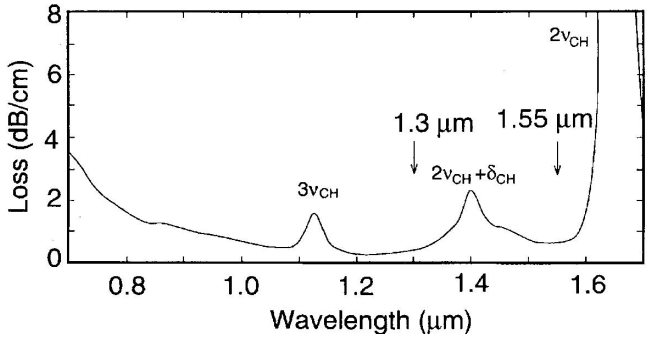

Figure 15.31. Loss spectrum for the film waveguide.

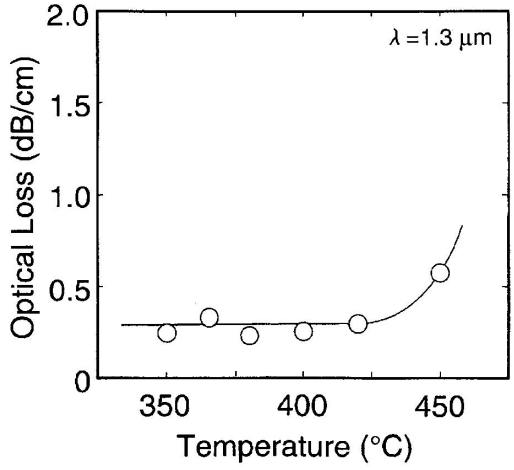

Figure 15.32. Optical loss of the film waveguide after heat treatment at various temperatures for 1 h

loss after heat treatment at various temperatures for 1 h. The small optical loss of 0.3 dB/cm was maintained after heating at temperatures of up to 420°C, but it began to increase after heating above 450°C. Single-mode operation was also maintained after heat treatment up to 420°C, but the output light changes from single-mode to multimode after heating above 450°C. [65] The optical loss of this waveguide does not increase after exposure to 85% RH at 85°C for more than 400 h, owing to the fact that the waveguide is fabricated with high-temperature curing and uses low-water-absorption polyimides.

(d) Bending Loss. This film waveguide is free-standing and has good flexibility. Figure 15.33 shows the optical loss of the waveguide after bending with various curvature radii. The low optical loss and single-mode behavior were maintained when the curvature radius was over 20 mm. At smaller curvature radii, the light is not fully confined to the core, so optical loss increases with decreasing radius.

(e) Birefringence. One of the features of this film waveguide is its very low in-plane/out-of-plane birefringence. We calculated the birefringence of the film waveguide to be a very low of 9×10^{-5} by the relationship between the phase retardation and the waveguide length (Senarmont method). This single-mode free-standing film waveguide has high thermal stability and good flexibility because it uses fluorinated polyimides as heat-resistant polymeric material.

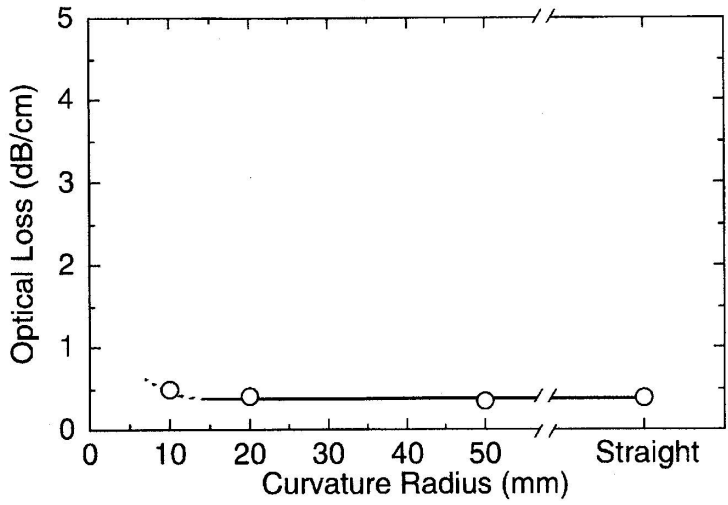

Figure 15.33. Optical loss of the film waveguide after bending with various curvature radii.

15.4.3.2. Polyimide Waveguides Using Electron Beam Irradiation

The refractive index of fluorinated polyimide can be controlled precisely by adjusting the electron beam irradiation dose as described in Section 3.2.2, and this feature can be exploited in fabricating polyimide optical waveguides. This section describes fluorinated polyimide waveguides fabricated by the direct electron beam writing method.[66-68]

The direct electron beam writing method is superior to the conventional method that uses reactive ion etching at several points. First, partial control of the refractive index and core width in the waveguides is possible, so device fabrication with fine structures is achieved easily. Second, waveguide fabrication is possible after optical devices have been positioned on the substrate. Moreover, this method is very useful for fabricating practical optoelectronic devices because the fabrication process can be simplified compared with reactive ion etching. Figure 15.34 shows a schematic diagram of the process for fabricating polyimide waveguides by direct electron beam writing, compared with the conventional method that uses reactive ion etching. A polyimide film is formed on a substrate by spin-casting and curing. The film is then exposed to an electron beam with an energy of 25 keV and a beam width of 0.2 μm. Line patterns are drawn for the core of the waveguides. Finally, a polyimide film is formed as an overcladding on this

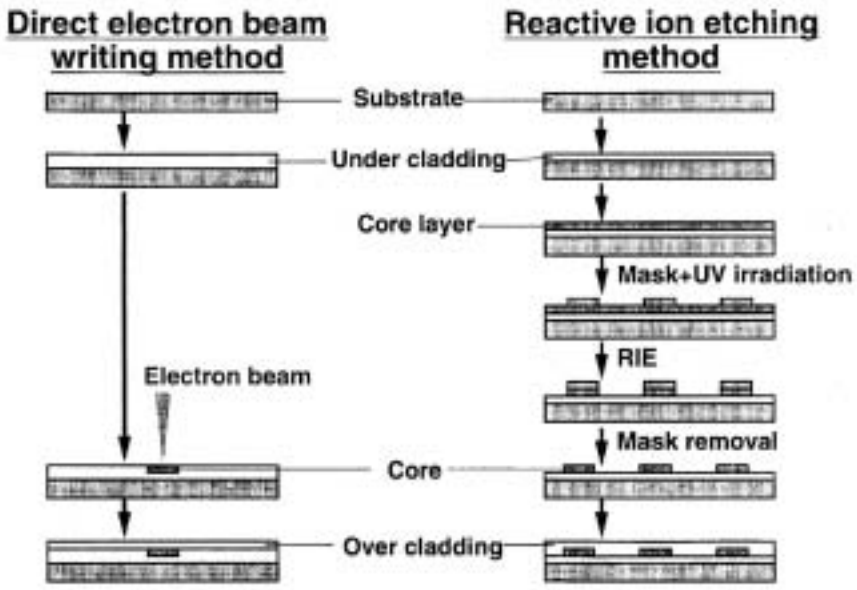

Figure 15.34. Schematic diagram of process for fabricating polyimide waveguides.

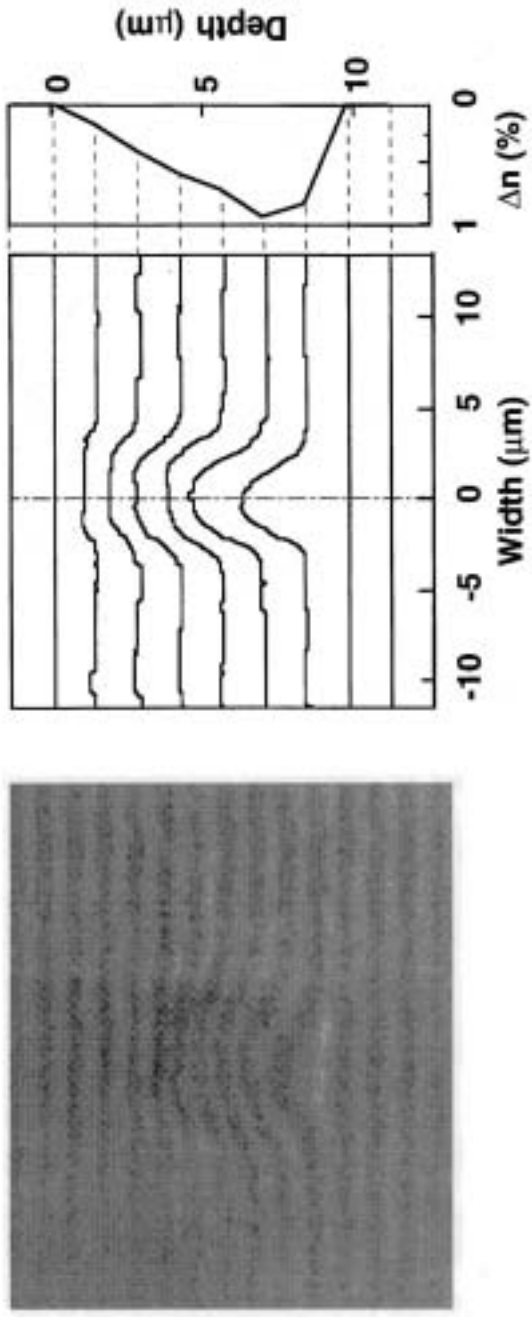

Figure 15.35. Interference micrograph and refractive index profile.

irradiated polyimide film by spin-casting and curing. This method reduces the number of steps in the fabrication process to less than half compared with the reactive ion etching method because the photolithography and reactive ion-etching processes are unnecessary.

The fabricated polyimide waveguides had core widths ranging from 7 to 12 μm, and lengths of 66 mm. Figure 15.35 shows the interference micrograph and the refractive-index profile of a waveguide fabricated with a dose of 1500 mC/cm² and a core width of 8 μm. The electron beam irradiated area was clearly observed. The maximum difference in refractive index between the core and cladding was found to be about 0.8%. The core depth was estimated to be about 9 μm. The depth profile of the refractive index distribution in the core region corresponded to the electron trajectory of Monte Carlo simulation in polyimide films.

Figure 15.36 shows near-field patterns for TE and TM polarized incident light at a 1.3-μm wavelength. The waveguide with a core width of 8 μm operates in a single mode, and the waveguide with an 11-μm core operates in multiple modes. The optical loss of the waveguides with a core width of 8 μm was 0.4 dB/cm for TE and 0.7 dB/cm for TM polarized incident light.

Buried channel-fluorinated waveguides consisting of a single material can be fabricated by direct electron beam writing, and we hope to develop novel optical devices by using this method.

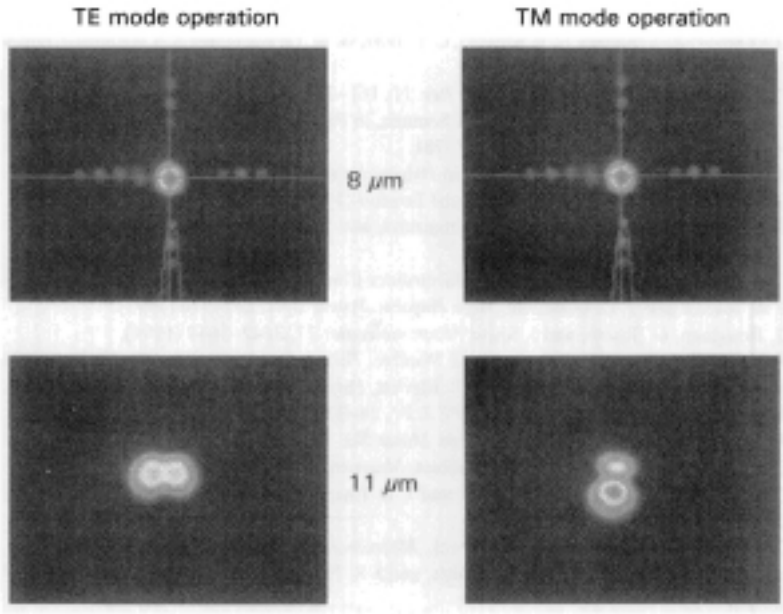

Figure 15.36. Near-field patterns for TE and TM polarized incident light at 1.3 μm

15.5. CONCLUSION

Fluorinated polyimides with high thermal stability were synthesized for optical applications. Introducing fluorine into polyimides achieves a high optical transparency in the visible and near-IR wavelength region, low water absorption, and low refractive index. Low-thermal-expansion polyimides with fluorinated side groups are also synthesized by introducing fluorine into polyimide molecules and by constructing rigid-rod structures. The refractive index can be precisely controlled by copolymerization of the high-fluorine-content 6FDA/TFDB polyimide and the low-fluorine-content PMDA/TFDB polyimide, and by electron beam irradiation. These copolyimides also make it possible to fit CTE to other materials such as Si, SiO_2, and metals by changing the 6FDA/TFDB content. The in-plane/out-of-plane birefringence can be also controlled by copolymerization, and the in-plane birefringence can be precisely controlled by the rigid-rod PMDA/TFDB polyimide. Optical devices for telecommunications, optical interference filters, optical waveplates, and single-mode waveguides were fabricated using these fluorinated polyimides and copolyimides, which have proved to be both attractive and practical polymeric materials for optical applications.

15.6. REFERENCES

1. C. E. Sroog, A. L. Endrey, S. V. Abramo, C. E. Berr, W. M. Edwards, and K. L. Olivier, *J. Polym. Sci. Pt. A 3,* 1373–1390 (1965).
2. C. E. Sroog, *J. Polym. Sci.: Macromol. Rev. 11,* 161–208 (1976).
3. D. R. Day, D. Ridley, J. Mario, and S. D. Senturia, in *Polyimides 2* (K. L. Mittal, ed.), Plenum Press, New York and London (1984), pp. 767–781.
4. H. Satou, H. Suzuki, and D. Makino, in *Polyimides* (D. Wilson, H. D. Stenzenberger, and P. M. Hergenrother, eds.), Blackie, Glasgow and London (1990), pp. 227–251.
5. S. Numata, S. Oohara, K. Fujisaki, J. Imaizumi, and N. Kinjo, *J. Appl. Polym. Sci. 31,* 101–110 (1986).
6. L.M. Ruiz, *Proc., 3rd Intern. SAMPE Electronics Conference,* June 20–22 (1989), pp. 209–217.
7. F. W. Mercer and T. D. Goodman, *High Perform. Polym. 3*(4), 297–310 (1991).
8. G. Hougham, G. Tesoro, and J. Shaw, *Macromolecules 27,* 3642–3649 (1994).
9. A. K. St. Clair, T. L. St. Clair, and W. P. Winfree, *Polym. Mater. Sci. Eng. 59,* 28–32 (1988).
10. A. K. St. Clair, T. L. St. Clair, and K. I. Shevket, *Polym. Mater. Sci. Eng. 51,* 62–66 (1984).
11. A. K. St. Clair and W. S. Slemp, *SAMPE J. 21,* 28–33 (1985).
12. A. K. St. Clair and T. L. St. Clair, *Polym. Mater. Sci. Eng. 55,* 396–400 (1986).
13. G. E. Husk, P. E. Cassidy, and K. L. Gebert, *Macromolecules 21* 1234–1238 (1988).
14. G. Hougham, G. Tesoro, A. Viehbeck, and J. D. Chapple-Sokol, *Macromolecules 27* 5964–5971 (1994).
15. G. Hougham, G. Tesoro, and A. Viehbeck, *Macromolecules 29,* 3453–3456 (1996).
16. J. P. Critchley, P. A. Grattan, M. A. Whitte, and J. S. Pippett, *J. Polym. Sci. Pt. A-1 10,* 1789–1807 (1972).
17. J. P. Critchley, P. A. Grattan, M. A. Whitte, and J. S. Pippett, *J. Polym. Sci. Pt. A-1 10,* 1809–1825 (1972).

18. T. Ichino, S. Sasaki, T. Matsuura, and S. Nishi, *J. Polym. Sci.: Polym. Chem. Ed. 28,* 323–331 (1990).
19. B. C. Auman, D. P. Higley, and K. V. Scherer, *Polym. Preprints 34*(1), 389–390 (1993).
20. F. W. Harris and S. L. C. Hsu, *High Perform. Polym. 1*(1), 3–16 (1989).
21. F. W. Harris, S. L. C. Hsu, and C. C. Tso, *Polym. Preprints. 31*(1), 342–343 (1990).
22. F. W. Harris, S. L. C. Hsu, C. J. Lee, B. S. Lee, F. Arnold, and S. Z. D. *Cheng, Mater Res. Soc. Symp. Proc. 227,* 3–9 (1991).
23. G. Hougham and G. Tesoro, *Polym. Mater Sci. Eng. 61,* 369–377 (1989).
24. M. K. Gerber, J. R. Pratt, A. K. St.Clair, and T. L. St. Clair, *Polym. Preprints. 31*(1), 340–341 (1990).
25. R. A. Buchanan, R. F. Mundhenke, and H. C. Lin, *Polym. Preprints. 32*(2), 193–194 (1991).
26. A. C. Misra, G. Tesoro, G. Hougham, and S. M. Pendharkar, *Polymer 33,* 1078–1082 (1992).
27. S. Trofimenko, in *Advances in Polyimide Science and Technology* (C. Feger, M. M. Khojasteh, and M. S. Htoo, eds.), Technomic Publishing, Lancaster and Base1 (1993), pp. 3–14.
28. B. C. Auman, in *Advances in Polyimide Science and Technology* (C. Feger, M. M. Khojasteh, and M. S. Htoo, eds.), Technomic Publishing, Lancaster and Base1 (1993), pp. 15–32.
29. B. C. Auman and S. Trofimenko, *Polym. Mater. Sci. Eng. 66,* 253–254 (1992).
30. A. E. Feiring, B. C. Auman, and E. R. Wonchoba, *Macromolecules 26,* 2779–2784 (1993).
31. M. E. Rogers, H. Grubbs, A. Brennan, R. Mercier, D. Rodrigues, G. L. Wilkes, and J. E. McGrath, in *Advances in Polyimide Science and Technology* (C. Feger, M. M. Khojasteh, and M. S. Htoo, eds.), Technomic Publishing, Lancaster and Base1 (1993), pp. 33–40.
32. W. D. Kray and R. W. Rosser, *J. Org. Chem. 42,* 1186–1189 (1977).
33. R.A. Dine-Hart and W.W. Wright, *Macromol. Chem. 143,* 189–206 (1971).
34. S. Ando, T. Matsuura, and S. Sasaki, *Polym. J. 29,* 69–76 (1997).
35. K. Furuya, B.I. Miller, L.A. Coldren, and R.E. Howard, *Electron. Lett. 18*(5), 204–205 (1982).
36. R. Reuter, H. Franke, and C. Feger, *Appl. Opt. 27*(21), 4565–4570 (1988).
37. C. T. Sullivan, *SPIE 994,* 92–100 (1988).
38. A.J. Beuhler and D.A. Wargowski, *SPIE, 1849,* 92–101 (1993).
39. S. Ando, T. Matsuura, and S. Sasaki, *ACS Symp. Ser. 537,* 304–322 (1994).
40. T. Matsuura, Y. Hasuda, S. Nishi, and N. Yamada, *Macromolecules 24,* 5001–5005 (1991).
41. T. Matsuura, M. Ishizawa, Y. Hasuda, and S. Nishi, *Macromolecules 25,* 3540–3545 (1992).
42. T. Matsuura, N. Yamada, S. Nishi, and Y. Hasuda, *Macromolecules 26,* 419–423 (1993).
43. T. Matsuura, S. Ando, S. Sasaki, and F. Yamamoto, *Macromolecules 27,* 6665–6670 (1994).
44. T. Oguchi, J. Noda, H. Hanafusa, and S. Nishi, *Electron. Lett. 27*(9), 706–707 (1991).
45. S. Ando, T. Sawada, and Y. Inoue, *Electron. Lett. 29,* 2143–2144 (1993).
46. T. Matsuura, S. Ando, S. Sasaki, and F. Yamamoto, *Electron. Lett. 29*(3), 269–270 (1993).
47. T. Matsuura, S. Ando, S. Matsui, S. Sasaki, and F. Yamamoto, *Electron. Lett. 29*(24), 2107–2108 (1993).
48. Y. Maki, and K. Inukai, *Nippon Kagaku Kaishi 3,* 675–677 (1972) [in Japanese].
49. H.G. Rogers, R.A. Gaudiana, W.C. Hollinsed, P.S. Kalyanaraman, J.S. Manello, C. McGowan, R.A. Minns, and R. Sahatjian, *Macromolecules 18,* 1058–1068 (1985).
50. S. Ando, T. Matsuura, and S. Sasaki, *Polymer 33*(14), 2934–2939 (1992).
51. Toray-DuPont Product Bulletin for Kapton polyimide film.
52. S. Ando, *Kobunshi Ronbunshu 51,* 251–257 (1994) [in Japanese].
53. F. W. Mercer and T. D. Goodman, *Polym. Preprints 32*(2), 189–190 (1991).
54. Y. Okamura, S. Yoshinaka, and S. Yamamoto, *Appl. Opt. 22*(23), 3892–3894 (1983).
55. Y. Y. Maruo, S. Sasaki, and T. Tamamura, *J. Vac. Sci. Tech. A 13*(6), 2758–2763 (1995).
56. Y. Y. Maruo, S. Sasaki, and T. Tamamura, Jpn. *J. Appl. Phys. 35,* 523–525 (1996).
57. Y. Y. Maruo, S. Sasaki, and T. Tamamura, *J. Vac. Sci. Tech. A 14*(4), 2470–2474 (1996).
58. K. Nakagawa, *J. Appl. Polym. Sci. 41,* 2049–2058 (1990).

59. S. Ando, T. Sawada, and Y.Inoue, *ACS Symp. Ser. 579,* 283–297 (1994).
60. S. Ando, T. Sawada, and Y. Inoue, *Polym. Preprints. 35,* 287–288 (1994).
61. T. P. Russell, H.Gugger, and J. D. Swalen, *J. Polym. Sci: Polym. Phys. Ed. 21,* 1745–1756 (1983).
62. N. Tomita, K. Sato, and I. Nakamura, *NTT Rev 3*(1), 97–104 (1991).
63. H. Takahashi, Y. Hibino, and I. Nishi, *Opt. Lett. 17,* 499–501 (1992).
64. Y. Inoue, Y. Ohmori, M. Kawachi, S. Ando, T. Sawada, and H. Takahashi, *Photon. Tech. Lett. 6,* 626–628 (1994).
65. T. Matsuura, S. Ando, T. Maruno and S. Sasaki, *CLEO/Pacific Rim '95,* Chiba, Jul. 11–14, FK2 (1995).
66. Y. Y. Maruo, S. Sasaki, and T. Tamamura, *Appl. Opt. 34*(6), 1047–1052 (1995).
67. Y. Y. Maruo, S. Sasaki, and T. Tamamura, *J. Lightwave Tech. 13*(8), 1718–1723 (1995).
68. T. Maruno, T. Sakata, T. Ishii, Y. Y. Maruo, S. Sasaki, and T. Tamamura, in *Organic Thin Films for Photonics Application Technical Digest Series, Vol. 21,* OSA/ACS Topical Meeting (1995), pp. 10–13.